Chem Soc Rev

Cite this: DOI: 10.1039/c2cs35254k

www.rsc.org/csr

TUTORIAL REVIEW

Building on architectural principles for three-dimensional metallosupramolecular construction†

Maarten M. J. Smulders, Imogen A. Riddell, Colm Browne and Jonathan R. Nitschke*

Received 11th July 2012
DOI: 10.1039/c2cs35254k

Over the last two decades the field of metallosupramolecular self-assembly has emerged as a promising research area for the development of intricate, three-dimensional structures of increasing complexity and functionality. The advent of this area of research has strongly benefited from design principles that considered the ligand geometry and metal coordination geometry, thus opening up routes towards rationally designed classical (Archimedean or Platonic) architectures. In this tutorial review, we will focus on more recent developments in the design and synthesis of three-dimensional suprastructures which have non-classical architectures (non-Archimedean/Platonic solids) and we will explicitly address the secondary effects responsible for their formation. Three classes of metallosupramolecular assemblies will be discussed: architectures formed through the combination of a single ligand and metal, heteroleptic structures and heterometallic structures. It is hoped that our exposition may suggest how different principles employed in these three classes of structures might be combined to create even greater complexity and potential for function.

Department of Chemistry, University of Cambridge, Lensfield Road, Cambridge, CB2 1EW, UK. E-mail: jrn34@cam.ac.uk
† Part of the centenary issue to celebrate the Nobel Prize in Chemistry awarded to Alfred Werner.

1. Introduction

In recent years a wide range of three-dimensional metallosupramolecular architectures has been synthesised;[1–3] some

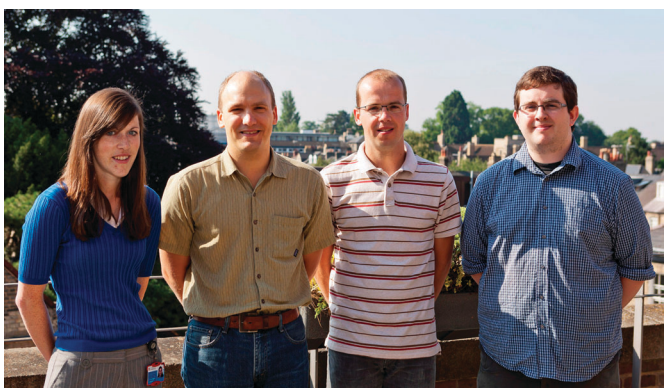

Imogen A. Riddell, Jonathan R. Nitschke, Maarten M. J. Smulders and Colm Browne

Maarten Smulders (second from right) was born in Liempde, the Netherlands. He received his MSc degree in Chemical Engineering and Chemistry in 2005 from the Eindhoven University of Technology, the Netherlands. From the same University he received in 2009 his PhD degree under the supervision of Prof. E. W. Meijer. In 2010, as a NWO Rubicon postdoctoral fellow, he joined the group of Dr J. R. Nitschke in Cambridge to work on self-assembled metal–organic cages. In October 2012 he joined the group of Prof. J. J. L. M. Cornelissen at the University of Twente, the Netherlands, as a NWO Veni fellow to work on responsive self-assembled materials.
Imogen Riddell (first from left) grew up in the Scottish Borders before moving to Glasgow to undertake an MSci degree in Chemistry. In 2009 she graduated from the University of Strathclyde having completed research projects under the supervision of Prof. P. Cormack and Prof. D. Graham, and industrial placements with Novartis and Pfizer. She is currently working towards her PhD in the group of Dr J. R. Nitschke, looking at the construction and application of novel supramolecular architectures using the subcomponent self-assembly methodology.
Colm Browne (first from right) was born in Dublin, Ireland. He remained in his home town to study Natural Sciences with a moderatorship in Chemistry at Trinity College Dublin, completing research projects with Prof. S. M. Draper and Dr W. Schmitt. In 2010 he moved to Cambridge to begin his PhD studies with Dr J. R. Nitschke, working on the synthesis of metallo-supramolecular architectures via subcomponent self-assembly.
Jonathan Nitschke (second from left) was born in Syracuse, New York, USA. He received his bachelor's degree from Williams College in 1995 and his doctorate from the University of California, Berkeley in 2001 under the supervision of T. Don Tilley. He then undertook postdoctoral studies with Jean-Marie Lehn in Strasbourg under the auspices of a US NSF fellowship, and in 2003 he started his independent research career as a Maître-assistant (fixed-term independent PI) in the Organic Chemistry Department of the University of Geneva. In 2007 he was appointed University Lecturer at Cambridge, where he now holds the position of Reader (Associate Professor, approximately). His research program investigates the self-assembly of complex, functional structures from simple molecular precursors and metal ions.

through careful design and others through serendipity, however, in each case an increased understanding of the design arguments governing the construction of the metal–organic architecture has been gained. Basic design principles learnt from nature[4] and solid geometry inspire the design of regular Archimedean and Platonic solids,[5] however, more complex architectures may be realised if the subtle secondary effects that govern non-covalent interactions are also taken into account.

Many of the metal–organic complexes reported have discrete void areas which impart unique properties to the structure leading to novel functions and applications:[6] modifying the chemical reactivity of guest complexes (stabilising reactive guests[7,8] or activating guests to react[9,10]), gas sequestration[11,12] or separation of species from a mixture.[13,14] These properties are modulated by the size and chemical properties of the binding pockets, which are in turn determined by the overall geometry of the metal–organic complex. Better control over three-dimensional architecture will result in complexes capable of performing processes akin to those observed in nature; encapsulating and modulating the chemical reactivity of guest molecules with greater size and structural complexity than those currently explored.

The programmed design of supramolecular structures can be guided by geometric design principles,[15–17] and as with synthetic organic chemistry, the rules governing the reactivity of many systems are understood such that a desired product can often be obtained. However, unlike classical organic synthesis, where reactions are performed one after the other under kinetic control, supramolecular synthesis relies on reactions which proceed under thermodynamic control, such that 'annealing' or 'error checking' processes may proceed to break down less stable products in favour of more stable ones. During these self-assembly processes, many reversible reactions may occur in parallel until the system reaches equilibrium, and thermodynamically stable products may be formed in near-quantitative yield.

In this tutorial review, we will focus on discrete, three-dimensional structures which have non-classical architectures (non-Archimedean/Platonic solids) and identify the subtle effects responsible for their formation. In our review we will limit ourselves to metal–organic architectures and will not discuss recent developments in the field of organometallic frameworks.[18–20] Moreover, we do not seek to provide an exhaustive review, as has been ably done recently by Stang and co-workers,[1] but instead try to identify common themes which underpin the deviation of structures from an architecture that would be predicted using geometric design principles. The review is split into three main sections: initially we examine unusual architectures formed through the combination of a single ligand and metal, followed by heteroleptic structures, which incorporate more than one ligand, and finally hetero-metallic structures, incorporating more than one metal ion.

2. Two-component architectures

A range of metallosupramolecular architectures have been created through combination of a single ligand and metal within one structure. Diverse architectures arise from, and can be rationalised by considering, changes in the metal-to-ligand stoichiometry, metal coordination geometry and ligand coordination vectors.[15] However, as increasingly complex supramolecular structures are realised, an improved understanding of some of the more subtle factors which determine the final architecture are being identified. In this section we aim to identify these secondary interactions and show how they influence the formation of structures comprised of a single ligand and metal environment.

A recent milestone in the field of supramolecular chemistry was marked by Fujita and co-workers, who in 2010 published the synthesis of a giant $M_{24}L_{48}$ rhombicuboctahedron, **1** (Fig. 1), and rationalised the formation of this species.[21] The self-assembly of **1** requires 72 components to come together in a highly organised manner to form an Archimedean solid with eight triangular and eighteen rectangular faces, forming a spherical complex with a huge internal void space. This group's previous work indicated that when a combination of rigid bent ligands (L) and square planar metal ions (M) were employed in the ratio M_nL_{2n} a roughly spherical polyhedron would result;[22] construction of the smaller 36-component cuboctahedron, **2**, employed a dipyridylfuran ligand with a bend angle of 127°. Fujita demonstrated, however, that changing the dipyridylfuran ligand for a structurally similar thiophene ligand, thereby increasing the ligand bend angle to 149°, brought about a major structural change as **1** was formed instead. When the authors mixed the thiophene- and furan-containing ligands in ratios from 9 : 1 to 1 : 9, in each case only the formation of a single product was observed. Ratios from 9 : 1 to 3 : 7 provided only $M_{24}L_{48}$ complex **1**, and at ratios below 3 : 7 the smaller $M_{12}L_{24}$ complex **2** was the sole product. Geometrically it was argued that a perfect rhombicuboctahedron having ideal edge angles of 135° was favoured enthalpically by the thiophene ligand, which would have to undergo substantial pinching and distortion in order to accommodate the entropically favoured $M_{12}L_{24}$ complex. In contrast, the furan ligand angle falls closer to the ideal edge angle for a cuboctahedron, 120°, and is therefore able to accommodate either geometry, but the smaller $M_{12}L_{24}$ species was preferred for entropic reasons. A more rigorous examination of this phenomenon was published more recently,[23] which extended the range of bidentate ligands employed, thereby subtly changing the angle formed between the two coordinating pyridine rings. The authors showed that within this family of ligands, ligand angles between 127–131° gave rise to $M_{12}L_{24}$ complexes whereas wider angles, 134–149°, gave rise to the larger $M_{24}L_{48}$ complex. Of particular note was the observation that under no conditions was a mixture of complexes **1** and **2** observed. The authors cite this as an example of molecular-level emergent behaviour whereby the small initial difference in the ligand bond angle is amplified to an incommensurate difference in the resultant structures.

The Fujita group has also explored the effects of using different square planar metal ions alongside the rigid dipyridylfuran ligand, specifically the replacement of kinetically labile Pd^{II}–pyridine bonds with kinetically inert Pt^{II}–pyridine bonds.[24] Upon addition of 2,2,2-trifluoroethanol (TFE), a strong hydrogen-bond donor, temporary labilisation of Pt^{II}–pyridine bonds was observed, which facilitated the self-assembly of $Pt_{12}L_{24}$ spheres. Upon removal of the TFE these spheres were shown to be more robust than their Pd^{II} counterparts. In the absence of TFE a complex mixture of products was formed which remained unchanged upon heating. This novel approach demonstrates the use of kinetically

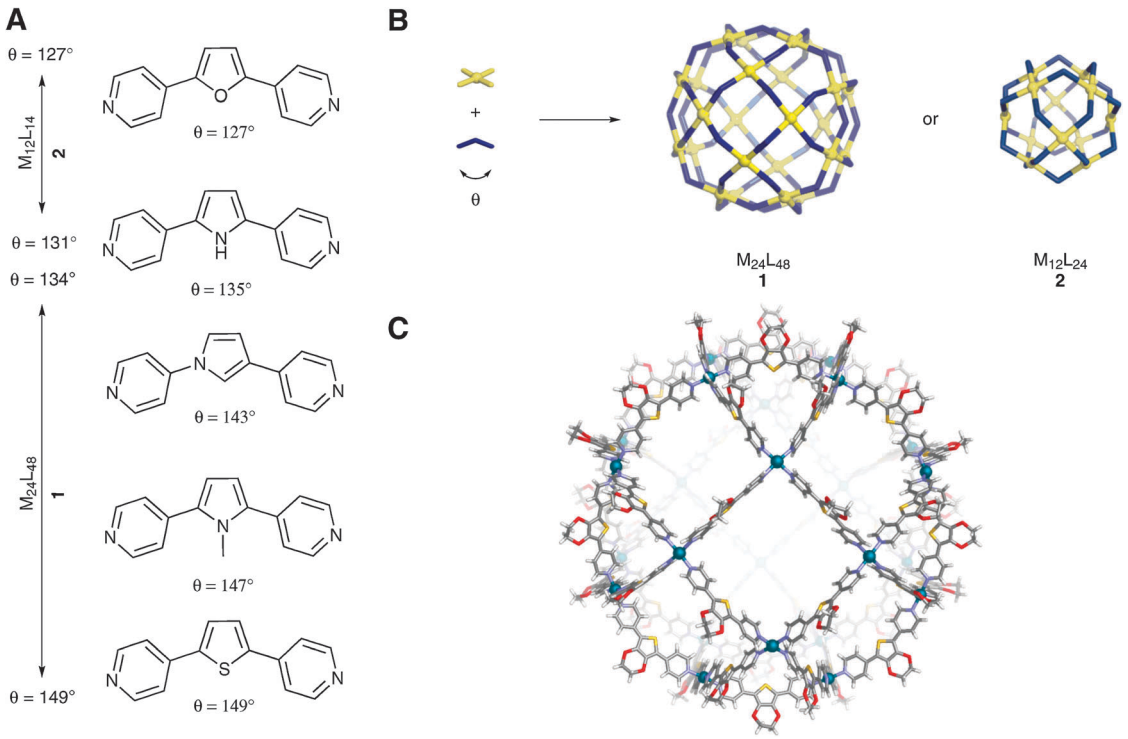

Fig. 1 (A) Ligands employed in the formation of complexes **1** and **2** displayed with their calculated bond angles. (B) Self-assembly of $M_{24}L_{48}$, **1** and $M_{12}L_{24}$, **2**, polyhedra; (C) Crystal structure of **1**.

inert metals in self-assembly reactions; temporary labilisation facilitates the error-checking mechanisms of self-assembly, ensuring formation of a single thermodynamic product, which is then rendered inert on removal of the labilisation agent (TFE). This methodology allows access to structures which are large, structurally complex and inert, properties not easily accessed otherwise.

In contrast to the edge-bridged methodology discussed above, in 2006 Lah and co-workers reported the synthesis and characterisation of two structurally related face-capped M_6L_8 truncated octahedral cages (Fig. 2).[25] Both of these complexes employed C_3-symmetric *facial* (*fac*) ligands connected by square planar Pd^{II} ions. The ligands employed consisted of a central phenyl ring linked at a 120° angle to three terminal pyridine rings through an amide bond. The torsion angle, ϕ, formed by the amide bond, between the terminal pyridyl groups of each arm and the central phenyl ring, generated the curvature necessary for the closure of these structures.

Crystallographic analysis indicated the existence of two conformational isomers of **5** in a 3 : 2 ratio. The major isomer derived from the ligand with *syn* conformation has a cavity volume of ~1600 Å^3; the minor isomer, having ligands with *anti* conformation, encloses a larger volume of ~1900 Å^3. ROESY spectra, however, indicated that only the major isomer with the *syn*-conformational ligand is observed in solution.

Changing the ligand from **3** to **4**, the authors showed that the 120° angle necessary for the structure could be incorporated not only through a *meta* substituted pyridine but also through the combination of an additional sp^3 carbon between the amide and a *para*-substituted pyridine. The resultant cage **6** was considerably larger, having a calculated volume of ~2200 Å^3.

Geometric design principles focus on coordinative interactions between organic ligands and metal ions, and do not consider interactions between ligands within an architecture, despite the structure-directing properties of secondary interactions. Several examples of energetically favourable interactions between aromatic rings within metal–organic cages have been reported by Ward and co-workers,[26] who have employed ligands incorporating linkers capable of adopting more than one conformation. As pointed out by Ward, the flexibility of this ligand precludes control of the relative orientations of the binding sites and subsequent synthesis of complexes and has resulted in many serendipitous findings.[26] In particular the incorporation of anthracene-9,10-diyl (**7**) and naphthalene-1,5-diyl (**8**) linkers into the backbone of the bis-bidentate ligand, gave informative results (Fig. 3).[27] In each case the ligands generated M_8L_{12} structures when coordinated to divalent metal ions with a preference for octahedral coordination geometry; however, the arrangement of the complex was shown to be ligand-dependent.

Ligand **7** produced architecture **10** (Fig. 3B) with divalent copper and zinc salts. From the X-ray crystal structure of the Zn_8L_{12} complex it was observed that the eight metal centres form an approximately cubic array with the twelve ligands lying along the Zn–Zn edges, with all metals adopting a *meridional* (*mer*) coordination geometry. Within complex **10** four metal centres on one face of the cube are connected by four bridging ligands in a circular helical array. The opposite face, which is generated by inversion, also incorporates a circular helical array, while the two helical faces are bridged by four perpendicular ligands. Most significantly, however, no aromatic π-stacking was observed within the crystal structure and no evidence of this structure could be found in the solution

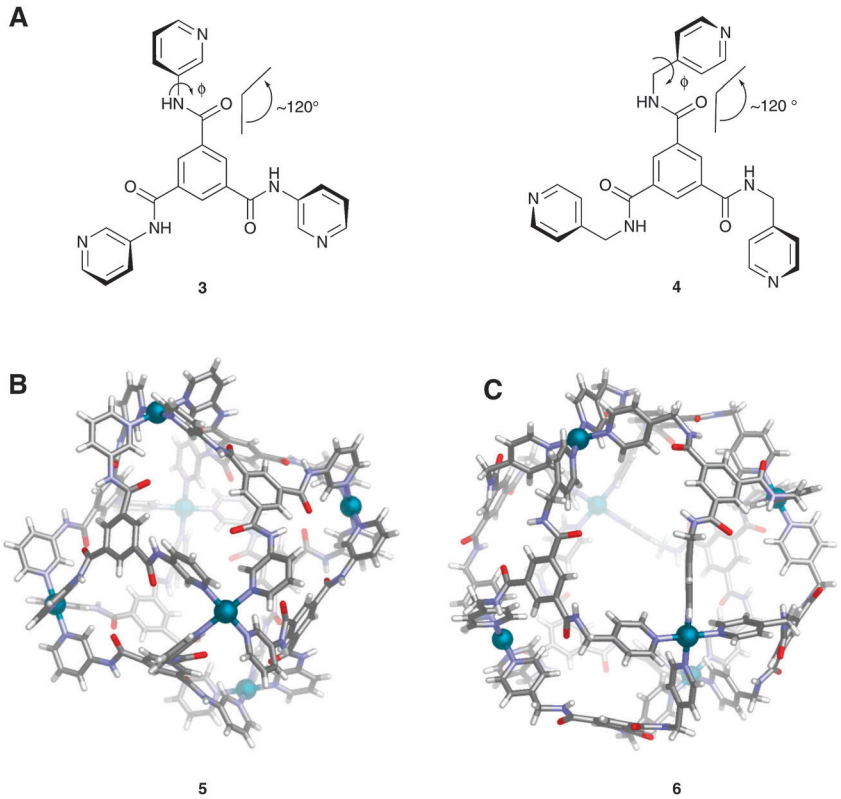

Fig. 2 (A) The structurally related ligands **3** and **4** employed in the formation of the truncated octahedral cages. (B) X-ray crystal structure of **5**, the M_6L_8 complex generated through the combination of **3** and Pd^{II} ions. (C) X-ray crystal structure of the corresponding structure, cage **6**, formed using **4** as the ligand.

state, either by ESI-MS or ^{1}H NMR. In contrast, ligand **8**, with divalent cobalt, nickel and cadmium salts, gave rise to **11** (Fig. 3C), which shows extensive π–π interactions within the cage. Unlike **10**, **11** could be characterised in the solution state by both ESI-MS and ^{1}H NMR as a consequence of the additional stabilisation provided by π–π interactions. As with **10**, the metal ions within **11** define the vertices of a cube, however in **11** all twelve of the electron-rich naphthyl units are sandwiched between two electron-poor pyridyl-pyrazole units resulting in a total of 24 donor–acceptor interactions. In addition, in contrast to complex **10** which contains only *mer* stereochemistry of the ligands around the metal centres, complex **11** incorporates two *fac* and six *mer* metal centres – these factors combined give rise to approximate (non-crystallographic) S_6 symmetry.

Using the isomeric ligand **9** a further unique M_8L_{12} structure was identified – a cuneane (Fig. 3D).[28] The cuneane is a topological isomer of a cube; the only one of 257 possible polyhedra with eight vertices which are each connected to three ligands. This results in a C_{2v}-symmetric 'wedge-shaped' structure containing two rectangular faces, two triangular faces and two roughly pentagonal faces. The authors report that chemical examples of such a structure are almost unknown and that it is surprising that they have not previously observed it as calculations predict the cuneane structure to be considerably more stable than the cubic isomer. As with the previous M_8L_{12} example, this structure again showed extensive π–π interactions, with its longest stack containing seven alternating electron-rich and electron-poor rings. Many of the structures observed with this class of ligand show extensive π-stacking, which plays a role in their stabilisation in solution and provides enthalpic compensation for the entropy lost when organising multiple components into larger architectures. Furthermore, the inclusion of both *mer*- and *fac*-coordinated vertices gives rise to a greater diversity of structures than could be observed for a single metal stereochemical configuration.

Recently we reported the synthesis and rationale for the construction of a $Co_{10}L_{15}$ pentagonal prism (Fig. 4).[29] The ligands in this complex, **15**, have significantly reduced flexibility compared to the ligands employed by Ward, although we also note favourable π-stacking interactions within **15** between the electron-rich toluidine and electron-poor pyridine rings wrapping around the outside of the structure. The observation that the same ligand can be accommodated in different architectures – having previously[13] been used in the formation of M_4L_6 tetrahedral cages with Fe^{II} – highlights once again that factors other than simply the ligands' coordination vectors and the preferred geometry of metals must be taken into consideration. In this case, replacement of Fe^{II} with Co^{II} brings about a significant structural rearrangement which may in part be linked to intrinsic properties of the metal; low-spin Fe^{II} has a tight coordination sphere with a preference for strict octahedral coordination. In contrast, high-spin Co^{II} has a slightly larger coordination sphere and a significant Jahn–Teller distortion. This distortion when propagated through the ligands breaks the threefold symmetry axis of the tetrahedron, thereby destabilising it relative to the Fe^{II} analogue. Furthermore, studies on model complexes showed that whereas Fe^{II} generates a statistical mixture of the *mer* and *fac* isomers, Co^{II} favours formation of

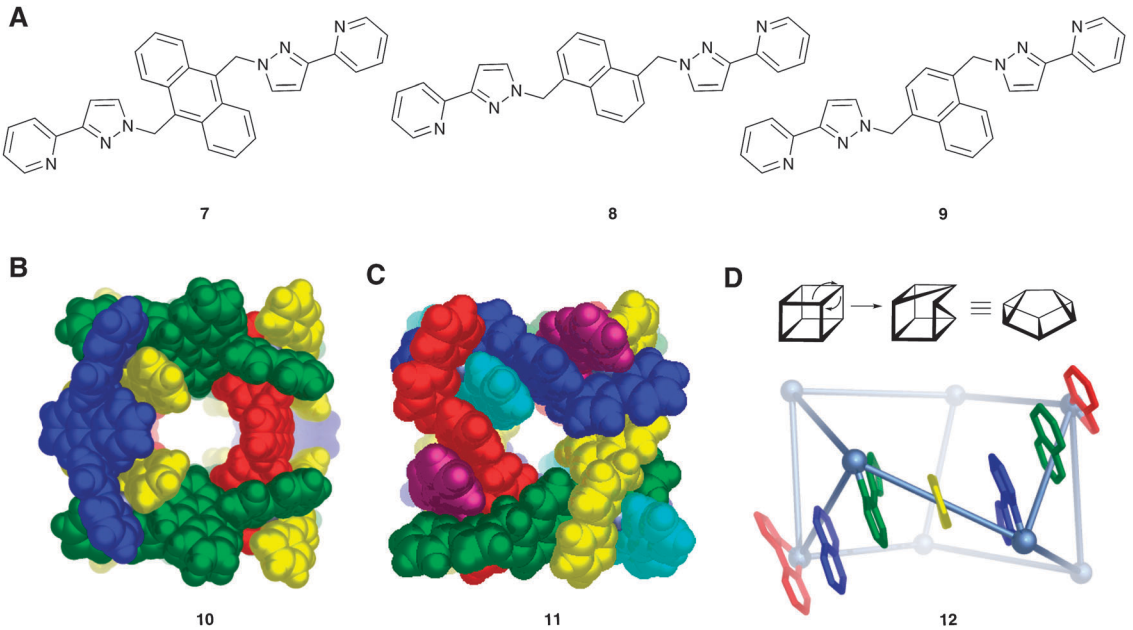

Fig. 3 (A) Structurally related ligands **7**, **8** and **9**. (B) X-ray crystal structure of the M_8L_{12} complex **10** formed from **7** and Zn^{II}. (C) X-ray crystal structure of the M_8L_{12} complex **11** formed from **8** and Co^{II}. (D) Scheme showing the structural rearrangement necessary to convert a cube to a cuneane, and below, X-ray crystal structure of the cuneane showing the extended π stack.

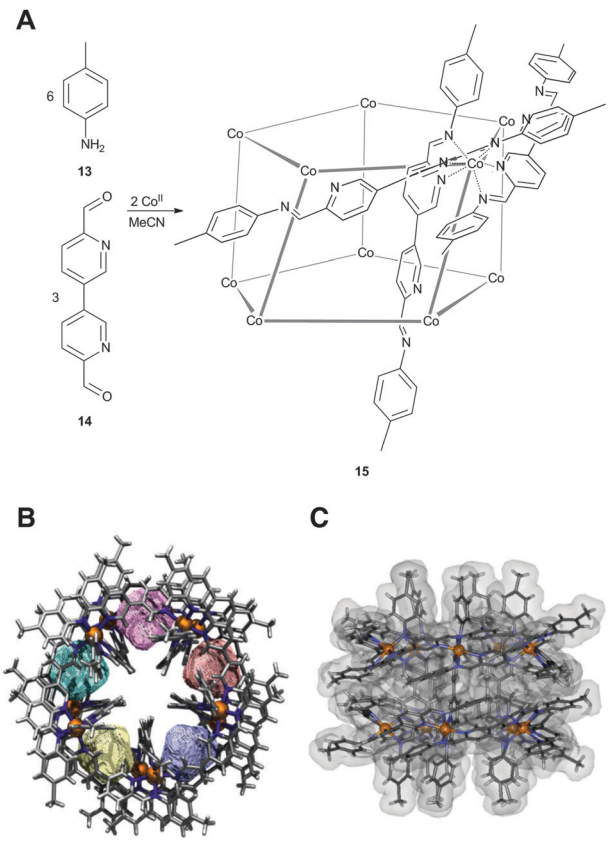

Fig. 4 (A) Subcomponent self-assembly of **15**. (B) Top-down view of the crystal structure showing modelled void pockets within **15**. (C) Edge-on space-filled view of the crystal structure.

the *mer* isomer. In contrast to the much more commonly encountered *fac* coordination of ligands around a metal centre, all ten Co^{II} centres in **15** are observed to have *mer* coordination.

In addition to the different templation roles played by the metal ions, anion templation is also observed to play a critical role in the formation of **15**. The presence of an anion which is a good size match for the pockets inside the barrel (ClO_4^-) will result in formation of **15**. However, when less well fitting anions are chosen (trifluoromethanesulfonate, OTf^-) the smaller M_4L_6 species is formed. Use of an intermediately sized anion (PF_6^-) resulted in the generation of a kinetic M_4L_6 product, which over time was observed to convert into the final thermodynamic product, **15**. Complex **15** employs a single ligand to fulfil two different roles; either serving as an equatorial ligand within the pentameric circular helicates, or acting as an axial bridging ligand between rings.

Helicates with sizeable internal cavities are rare; one notable example is that of Cui and co-workers who recently published a homochiral quadruple-stranded helicate which undergoes enantioselective host–guest chemistry.[30] Complex **17** is comprised of two halves, the top and bottom section each contain two five-coordinate trigonal bipyramidal Zn^{II} centres enclosed within the N_2O_2 pockets and linked by the phenolato O atoms. Two of these units are then linked through an additional four equatorial Zn^{II} centres which coordinate two of the peripheral pyridyl groups of the ligand and two chloride anions each (Fig. 5).

The homochiral salan ligand was shown to be essential for the formation of **17**; when the equivalent racemic ligand was used under identical conditions only the dimeric Zn_2L_2 complex was observed to form. In this case each dimeric unit was observed to contain two opposite-handed ligands, which resulted in the four pyridyl groups that make up the equatorial plane of the helicate being directed towards different faces of the now almost planar Zn_2O_2 core thereby disfavouring the formation of **17**.

X-ray crystallography confirmed the formation of **17** – a porous helicate cage containing a chiral binding pocket,

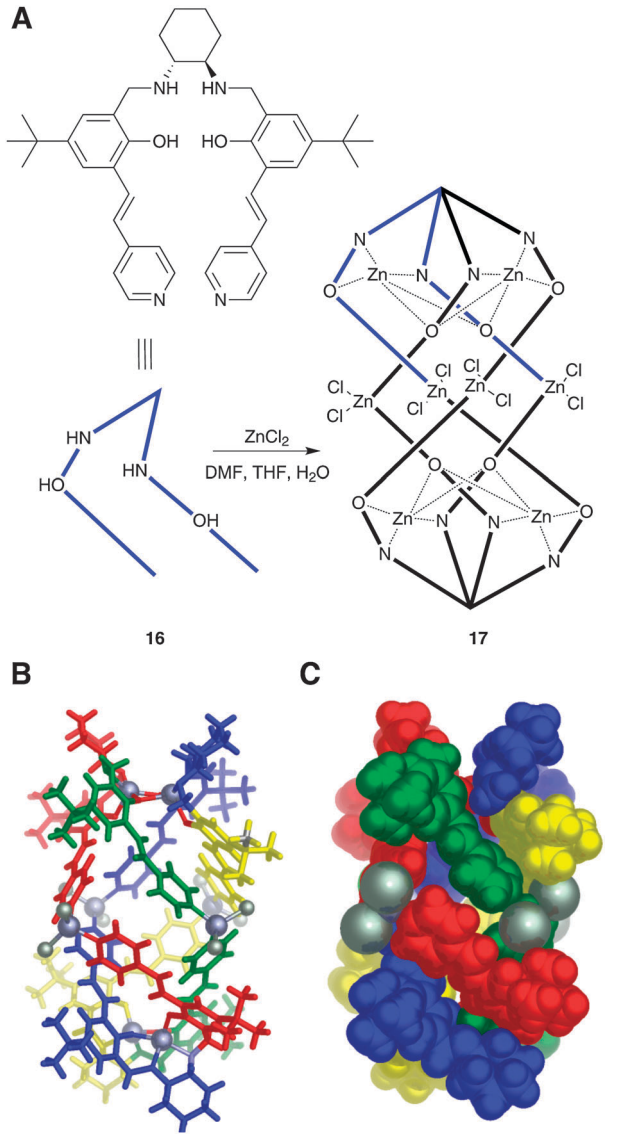

Fig. 5 (A) Self-assembly reaction of ligand **16** into complex **17**. (B) Ball and stick representation of X-ray crystal structure of **17** showing internal void space. (C) Space-filled representation of the X-ray crystal structure of **17**.

chirotopically arranged NH functional groups and wide apertures – suggesting the suitability of the system for enantioselective guest recognition and separation. Fluorescence measurements were used to assess the host–guest binding capabilities of **17** and the amino acids alanine, phenylalanine and valine were shown to bind enantioselectively. No enantioselectivity was reported with the free ligand.

Few metal–organic polyhedra which incorporate threaded, mechanically locked motifs are known;[31] one such example is complex **19** (Fig. 6A).[32] This remarkable dimeric assembly of interpenetrated cages formed spontaneously upon prolonged heating of a sample of the monomeric capsule. Complex **19** was observed to bind a single tetrafluoroborate anion between the central two Pd^{II} centres and could bind an additional two smaller anions with high affinity, between the outermost Pd^{II}–Pd^{II} stacks. The formation of this complex and the extremely high binding constant for the incorporated anions may be rationalised by considering the positive Coulombic interactions between the closely associated Pd^{II} and BF_4^- ions, suggesting guest templation of the host framework. The structure-directing properties of guest molecules, in particular of counterions, are beneficial to consider during the design of supramolecular systems. In addition to the anionic effects mentioned above, both the π–π interactions observed between the ligands and the entropic benefits from the release of trapped solvent upon dimerisation, appear to contribute to the formation of **19**.

Another mechanically interlocked complex of note is the Solomon cube **21** (Fig. 6B).[33] This unusual M_4L_4 structure

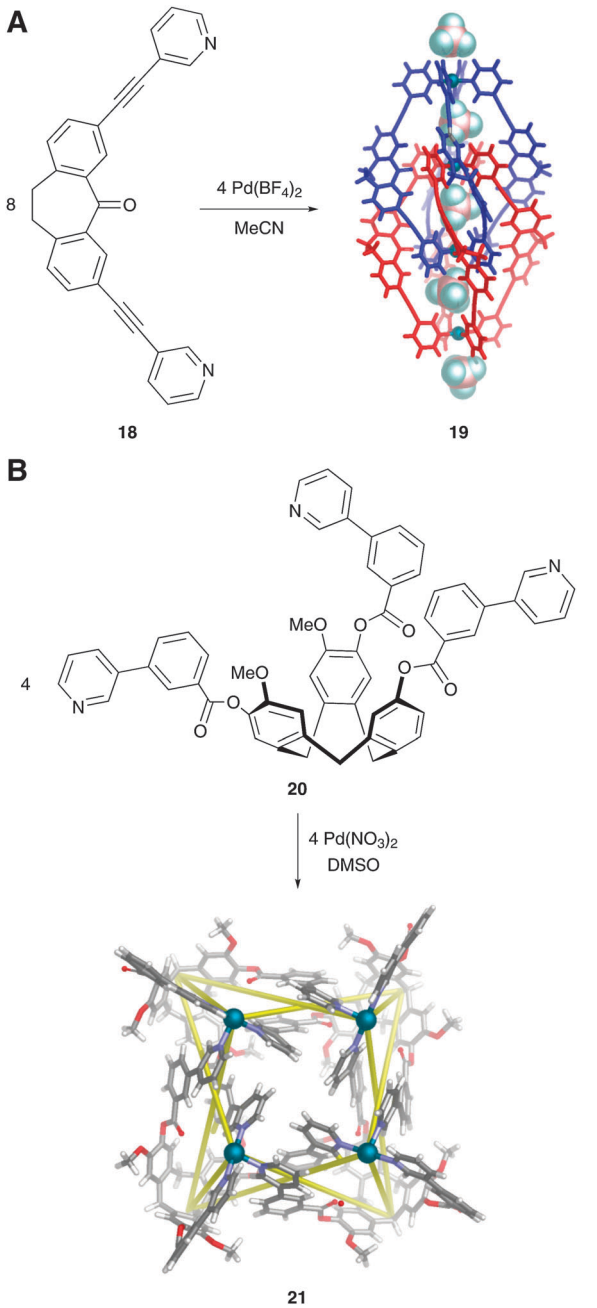

Fig. 6 (A) Self-assembly of ligand **18** into complex **19**; the X-ray crystal structure of **19** is depicted, showing encapsulated anions. (B) Solomon Cube complex **21**.

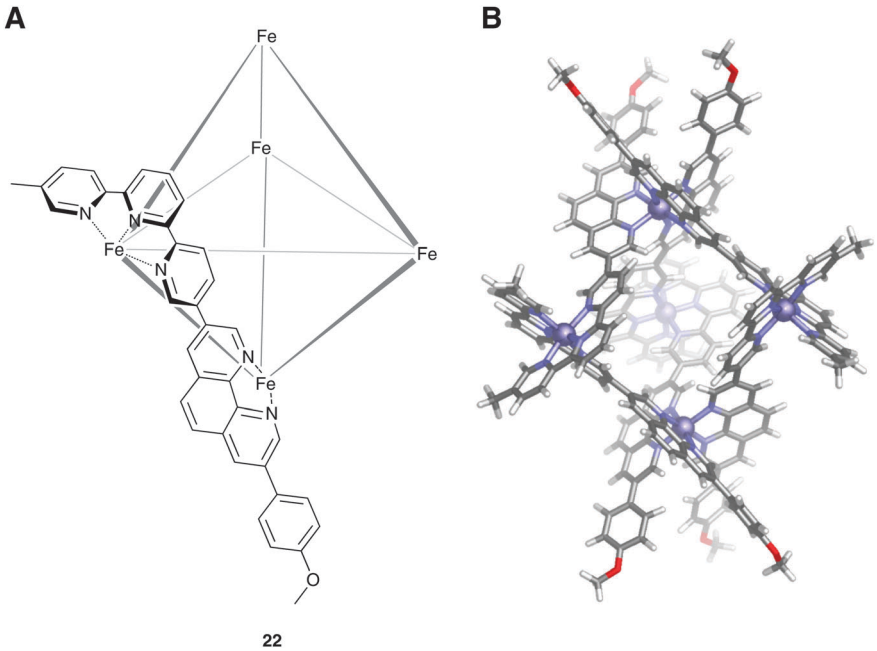

Fig. 7 (A) Schematic representation of **22**, showing only one ligand for clarity. (B) DFT-minimised model of **22**.

incorporates rigid yet rotatable cyclotriguaiacylene (CTG) units with metal-binding pyridyl groups in the 3-position. When a similar ligand with pyridyl groups in the 4-position was employed, the topologically trivial M_6L_8 complex was isolated. In addition to this geometric constraint, favourable π-stacking is again observed to play a crucial role in the formation of **21**: in the crystal structure pairs of interlocked phenyl-pyridyl ligand side arms are shown to overlap favourably.

Another method employed to generate complex metallo-supramolecular structures is the use of heteroditopic ligands, incorporating two different functionalities with orthogonal binding modes, in a single ligand. Most commonly this method is employed in heterometallic systems where different metals will preferentially associate with one or other of the functional groups, as discussed in the final section of this review. However, Tatay and co-workers have designed a heteroditopic linear ligand containing a tridentate 2,2′:6′,2″-terpyridine (terpy) moiety and a bidentate 1,10-phenanthroline (phen) moiety which undergoes self-assembly in the presence of solely Fe^{II} ions (Fig. 7).[34]

The design and synthesis of asymmetrical ligands is generally more labour intensive than the preparation of their symmetrical counterparts, but asymmetrical ligands can give rise to architectures not available using symmetric ligands. Simple linear homoditopic bis-bidentate bridging ligands can give rise to polyhedral cages, where the ligands bridge the edges and the metal ions define the vertices. In contrast, when homoditopic bis-terdentate ligands are combined with octahedral metals, they generally give rise to planar metallocycles[35] or 2-stranded helicates.[36] The combination of these two motifs into one ligand, and the reaction of this ligand with Fe^{II}, however, gave rise to a novel Fe_5L_6 complex, **22**. It was hypothesised that the metals and ligands were organised into a trigonal bipyramid where each of the three equatorial vertices are occupied by two terpy units, whereas the two axial vertices are coordinated to three phen units, thereby fully saturating all the ligand binding sites and fulfilling the coordination preference for octahedral Fe^{II}. No single-crystal X-ray data were supplied for this complex, however, 1D and 2D ^{1}H NMR, ESI-MS and DFT modelling all supported formation of the proposed structure. The coordination preferences of the metal were shown to play an important role in the construction of **22**, as when the same ligand was employed in the presence of Cu^{II} ions, a hexagonal metallamacrocycle was isolated in place of **22**. Furthermore, when Co^{II} or Zn^{II} were employed in place of Fe^{II} no single product could be identified from the reaction mixtures. The authors attribute this different behaviour to the stronger binding between the Fe^{II} and the ligands.

The effect of a template molecule provides another contributing factor in the formation and stabilisation of complex supramolecular architectures, as discussed in the case of **15**. Another striking example was reported by Anderson and co-workers, who demonstrated the principle of Vernier templation in the formation of a 12-porphyrin nanoring, **23**.[37] In 1998 Bregant and co-workers reported the first molecular Vernier complex[38] whereby two three-fold and three two-fold H-bonding assemblies combined to form a single pentameric complex. Expanding this concept to non-linear systems facilitated the design of **23**, the size of which was programmed through a combination of the template and the oligomeric precursors; in this case, a hexylpyridyl template and three linear porphyrin tetramers (Fig. 8A). After templation, palladium-catalysed oxidative coupling was used to complete the nanoring, which remained held in a figure of eight motif until the two hexapyridyl templates were released upon addition of excess competing pyridine. The final porphyrin nanoring could also be prepared using classical template synthesis, employing a synthetically-challenging dodecapyridyl template (Fig. 8B). The advantage of using a Vernier template is the reduced synthetic effort involved in making the smaller and simpler

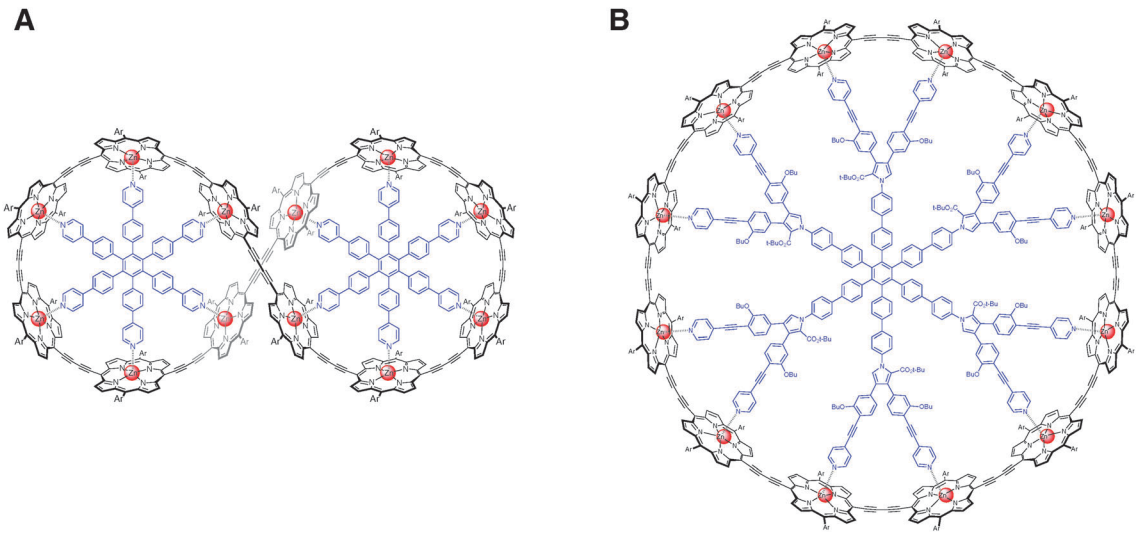

Fig. 8 (A) Complex **23** *via* Vernier template. (B) Complex **23** using a classical template synthesis.

hexylpyridyl templates. In the absence of either of the templates only linear polymers were formed.

Further expanding the concept of Vernier templation the same group has recently published a follow-up paper detailing the two possible routes to formation of the related 24-porphyrin nanoring.[39] The synthesis of which may be performed either through coupling three linear porphyrin octamers in the presence of four hexapyridyl templates or by coupling four linear porphyrin hexamers in the presence of three octapyridyl templates.[39] This novel templation effect shows obvious potential for the formation of larger supramolecular complexes; we look forward to the further development of this methodology and the novel supramolecular structures it gives rise to.

3. Heteroleptic structures

An alternative strategy to create more complex architectures entails the use of more than one ligand coordinating to a single metal ion, resulting in heteroleptic assemblies. Recently, Schmittel and co-workers have reviewed metal-coordination-driven dynamic heteroleptic architectures, although their emphasis was on assemblies of lower dimensionality (*i.e.* one- and two-dimensional architectures).[40] As will be discussed in this section, the factors explored by Schmittel *et al.* as contributing to the formation of heteroleptic species are, amongst others, also operative in the formation of three-dimensional heteroleptic architectures.

One of the first examples of a heteroleptic three-dimensional metal–organic architecture was reported by Lehn and co-workers in 1993,[41,42] who reported that the slow addition of a Cu^{I} salt (6 equivalents) to a mixture of 3 equivalents of rigid quaterpyridine ligand **24** and 2 equivalents of the hexaazatriphenylene **27** ligand in acetonitrile resulted in the formation of complex **28** (Fig. 9).[41] Model studies, in which a Cu^{I} salt was added to a mixture of 3 equivalents of a bipyridine (bpy) derivative and 1 equivalent of **27**, showed that initially all the Cu^{I} coordinated to the bpy to form $Cu^{I}(bpy)_2$ complexes until all bpy was consumed. Further addition of Cu^{I} resulted in breakdown of the $Cu^{I}(bpy)_2$ complexes in favour of formation of the heteroleptic Cu^{I} complex **28** by coordination to the more weakly-binding ligand **27**, which at 3 equivalents of Cu^{I} became the only reaction product. The creation of the heteroleptic Cu^{I} complexes thus satisfies the principle of maximum site occupancy, defined as the *evolution of the system toward the species or the mixture of species that presents highest (or full) occupancy of the binding sites available on both the ligand and the ions*.[43]

In a later contribution Lehn *et al.* showed how the same heteroleptic coordination motif allowed for the formation of multicompartmental architectures. To this end, instead of the quaterpyridine ligand, a linear tris(bpy) (**25**) or tetrakis(bpy) (**26**) was combined with ligand **27** and a Cu^{I} salt in the appropriate ratio, thus yielding complexes **29** and **30**, respectively (Fig. 9). Because two types of ligands make up the complex, by changing the nature of only one of the two ligands, the assembly could be extended in one dimension, thus increasing the number of compartments in the assembly. X-ray crystal structure determination unequivocally confirmed the structures of both **29** and **30**, and also revealed the presence of four (in the case of **29**) or six (in the case of **30**) PF_6^- anions in the complex's cavities. The formation of these complexes is driven by a maximisation of site occupancy, as well as entropic considerations, whereby the smallest number of components is chosen that can form a discrete supramolecular entity satisfying maximum site occupancy.

If the preparation of a heteroleptic metal–organic capsule relies on two ligands with similar dimensions and functional groups, measures should be taken to ensure that the heteroleptic complex is favoured over the corresponding homoleptic complexes. One such method entails the addition of a template that can selectively stabilise the heteroleptic complex(es). Fujita and co-workers employed this strategy to control the ratio of homoleptic *versus* heteroleptic complexes for the dynamic library of three cages prepared from a mixture of tridentate ligands **32** and **33** and Pd^{II} complex **31**.[44] The structural similarity between ligands **32** and **33** resulted in the formation of the two homoleptic capsules, **34** and **35**, as well as heteroleptic capsule **36** (Fig. 10). In the absence of a guest, the ratio of homoleptic *versus* heteroleptic cages was found to be 6 : 4. The addition of two guests with complementary sizes

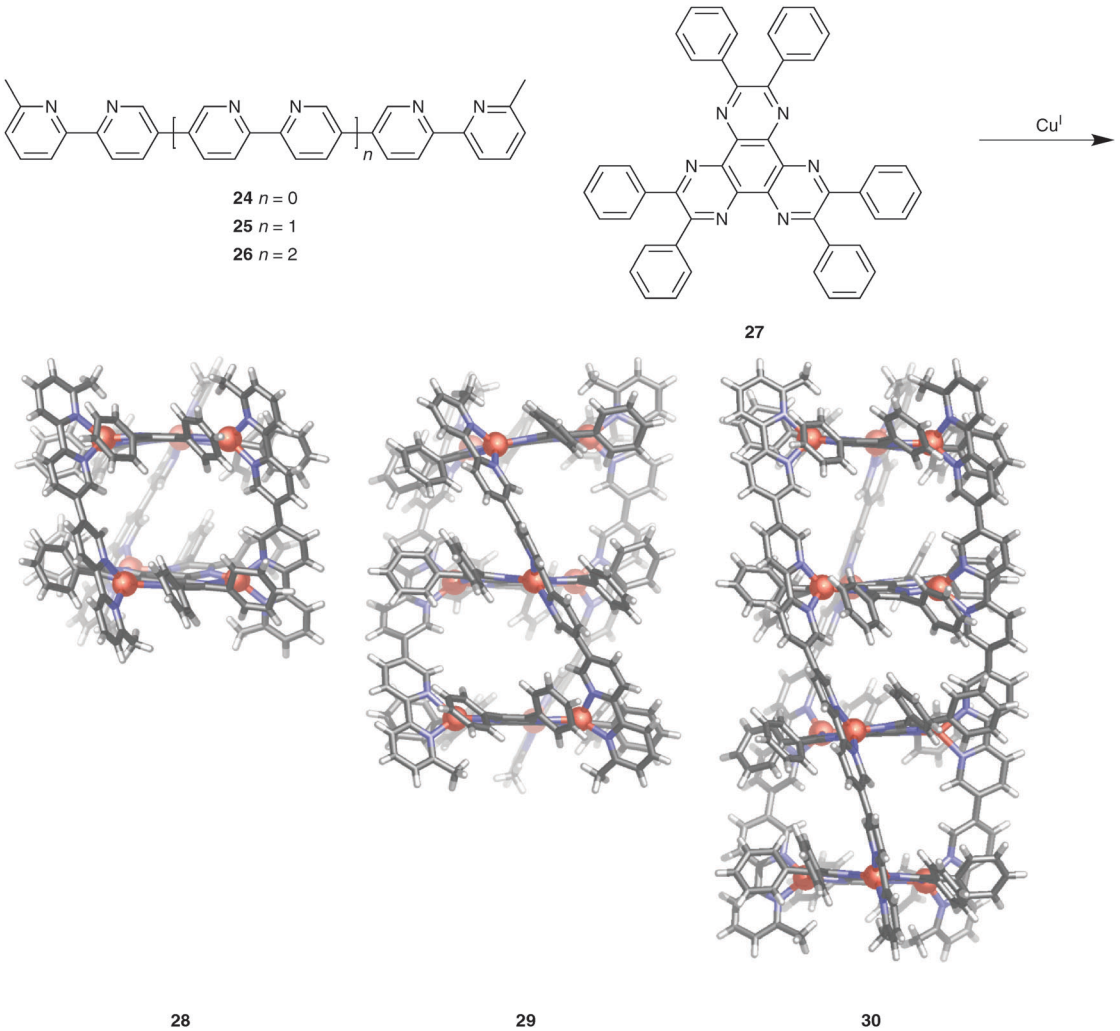

Fig. 9 Synthesis of the heteroleptic cylindrical architectures **28–30** containing one, two and three internal cavities, respectively.[41,42]

and shapes to each of the homoleptic cages, *i.e.* benzene-1,3,5-tricarboxylic acid for the flatter cage **35** and adamantan-1-ol for the bulky cage **34**, led to exclusive formation of the homoleptic species. In contrast, addition of a 'medium-sized' guest, *e.g.* CCl_4, $CBrCl_3$ or cycloheptane, was found to favour the heteroleptic cage, **36**, shifting the ratio of homoleptic *versus* heteroleptic to 3 : 7.

Fujita and co-workers also reported the crucial role templation can play in the selective formation of a heteroleptic, trigonal prismatic cage.[45] Only when components **37–39** were combined in a ratio of 6 : 2 : 3 in D_2O in the presence of (excess) template hexamethoxytriphenylene **41**, could trigonal prismatic capsule **40** be formed (Fig. 11). Crystallographic analysis of **41**⊂**40** revealed that the aromatic guest stabilises the cage by π–π interactions (the face-to-face distance between the triazine plane and the triphenylene plane was found to be 3.3 Å), which was reflected in the observation of a charge transfer band in the UV/vis spectrum.

In the absence of the template, homoleptic complexes **42** and **43** were observed, together with uncharacterised products. Both of the homoleptic complexes **42** and **43** are thermodynamically stable in each other's absence, as evidenced by separate studies in which Pt^{II} complex **37** was mixed with ligand **38** or **39**, respectively.[46] The exclusive formation of heteroleptic cage **40** is thus driven by a strong stabilising effect due to templation. Although the formation of **40** required a template, the cage was found to be sufficiently stable that after removal of the template, the cage persisted in solution. The empty cage was then able to encapsulate other neutral aromatic guests, such as pyrene.

In subsequent research, the height of similar trigonal prismatic cages was varied by changing the length of the bipyridine linkers that act as the pillars in the prismatic cages (Fig. 12).[47] As an alternative method to prepare the heteroleptic cages, instead of using an aromatic template molecule, methyl substituents *ortho* to the N atom in the pyridine ring could be introduced to prevent formation of the homoleptic cages by steric means.

This modular approach enabled Fujita *et al.* to tune the height of the trigonal prismatic cage to accommodate particular guests, allowing the investigation of various phenomena inside the cage's cavity, ranging from spin crossover[48] to the formation of [$m \times n$] metal ion arrays,[49] electron transport through aromatic stacks[50] and encapsulation of discrete stacks of polarised aromatic guests.[51]

By modification of only one of two types of ligands it is thus possible to modify the size of the cage in only one dimension (*i.e.* the base of the trigonal prism is unchanged while the

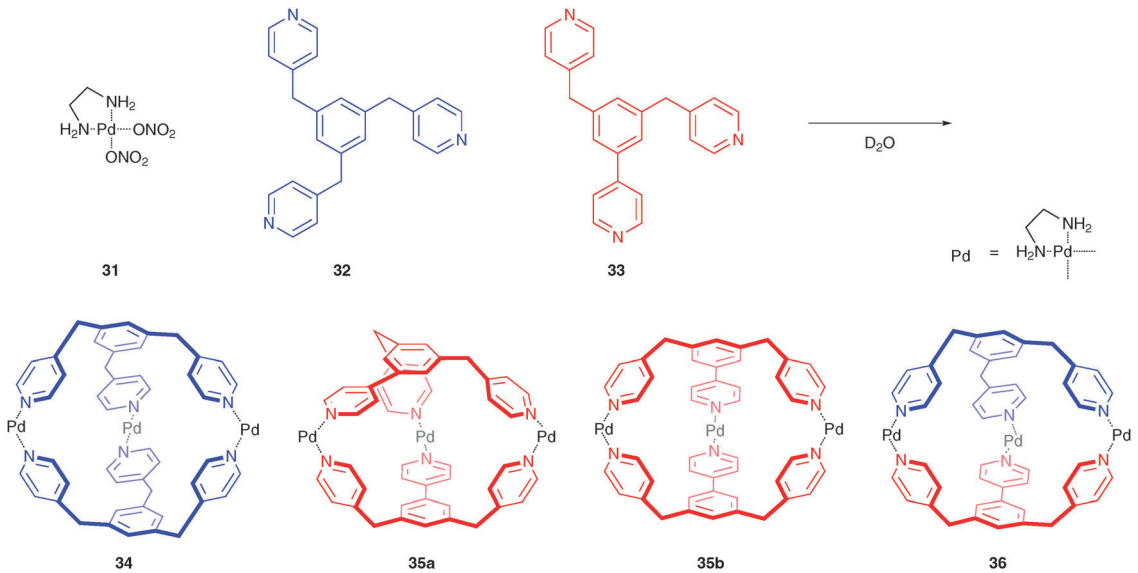

Fig. 10 Homo- and heteroleptic Pd^{II}-linked capsules prepared from ligands **32** and **33**. The homoleptic capsule derived from **33** is present as two different structural isomers: **35a** and **35b**.[44]

height is increased). In contrast, modification of a cage in one specific dimension is not possible for homoleptic cages, where changes in the ligand will affect the cage in all three dimensions.

Instead of changing the distance between the top and bottom face of the trigonal prism by modification of the length of the pillar, Therrien and co-workers varied the steric bulk of the pillar ligands as a means to control the guest release kinetics (Fig. 13).[52] In previous work Therrien *et al.* had reported how η^6-coordination of arene ligands can be used to control the accessibility of coordination sites on a metal ion (ruthenium).[53] Six of these (η^6-arene)ruthenium metal centres could thus bring together two trigonal tris(4-pyridyl)triazine panels (**38**) and three oxalato (or dichloro) bridges, resulting in

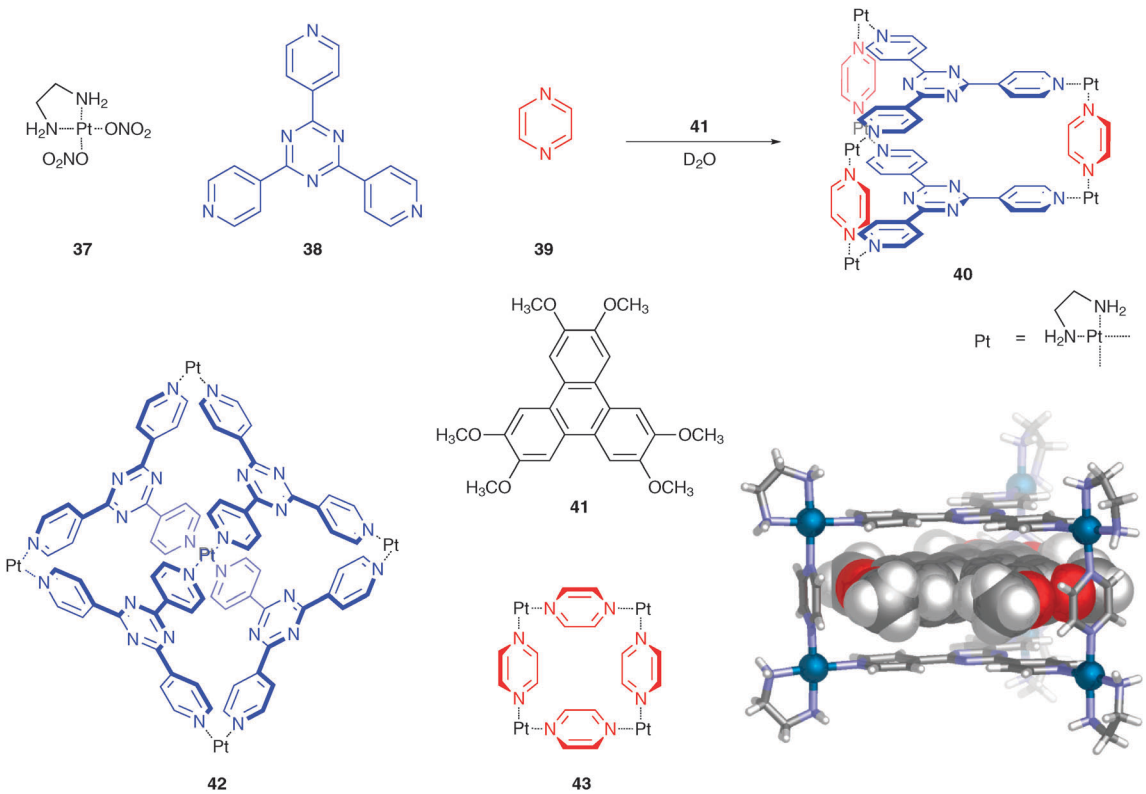

Fig. 11 Template-directed synthesis of heteroleptic, trigonal prismatic cage **40**. In the absence of template **41** homoleptic complexes **42** and **43** are formed. Bottom right the crystal structure of **40** is shown, with the template **41** residing in the cage's interior.[45]

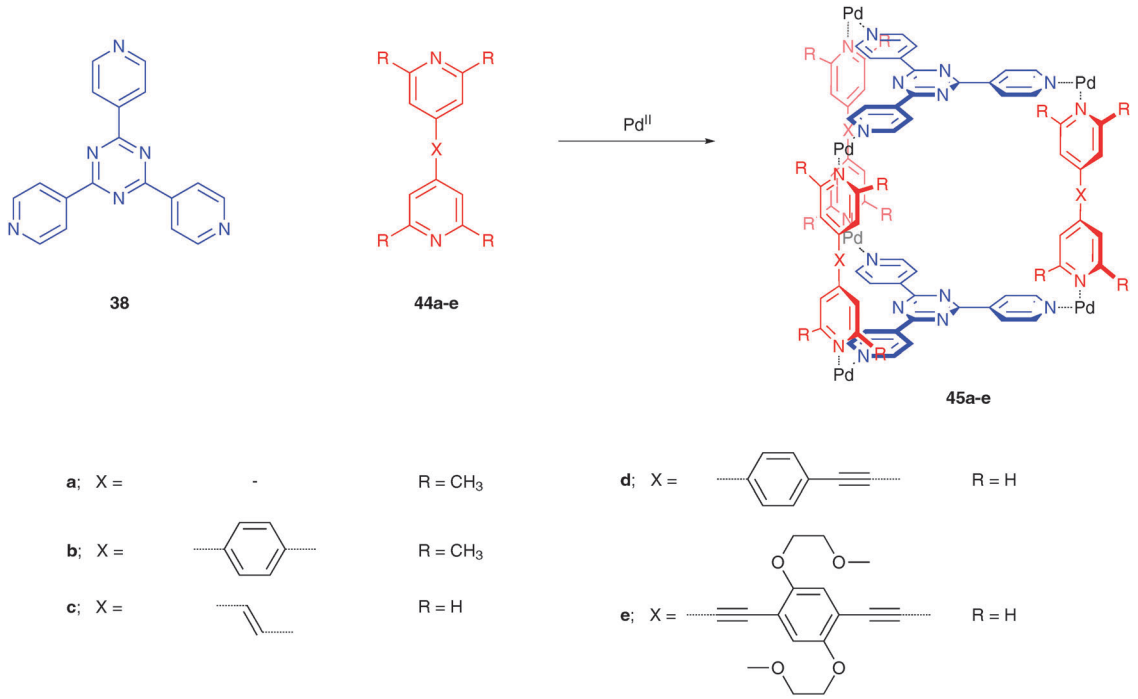

Fig. 12 Overview of the different heteroleptic, trigonal prismatic cages prepared from tris(4-pyridyl)triazine **38** and linear bipyridine linkers **44** in the presence of Pd^{II}.[47]

a trigonal prismatic cage. This self-assembly process is driven by a maximisation of site occupancy and does not require the presence of a template. In addition to a range of aromatic guests,[54] $Pd(acac)_2$ and $Pt(acac)_2$ (acac = acetylacetonato) could also be encapsulated in the prismatic cage, which allowed the use of the cage as a drug delivery vehicle in aqueous conditions; a methodology referred to by the authors as a 'Trojan Horse' strategy.[55]

To obtain better control over the release properties of the hexanuclear prismatic cages, Therrien and co-workers prepared a series of cages, **49–51**, with a similar cavity volume, but with differently sized portals (Fig. 13). Molecular dynamics simulations revealed that the portal dimensions for the three cages decreased from 10.2 × 7.4 $Å^2$ to 9.0 × 7.4 $Å^2$ to 7.8 × 7.4 $Å^2$ for the cages with increasing linker width.

The uptake and release kinetics of a pyrene derivative and of $Pd(acac)_2$ were investigated for the three different cages. It was first of all observed that both in acetonitrile and DMSO the strength of binding of the pyrene guest decreased with increased linker width. As this class of hexanuclear ruthenium cages can be used as a drug delivery vehicle (see above),[55] the effect of portal size on the release kinetics of both the pyrene guest and the $Pd(acac)_2$ was investigated by cytoxicity studies in A2780 ovarian cancer cells. A correlation between the portal

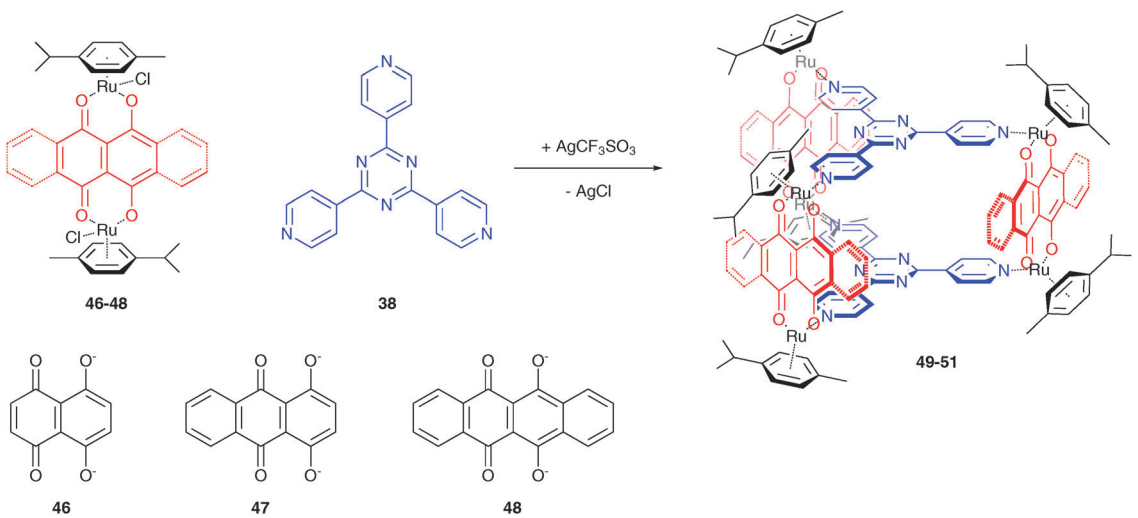

Fig. 13 Heteroleptic Ru^{II}-based cages **49–51** whose guest release properties are controlled by the steric bulk of the ligands **46–48** from which they are prepared.[52]

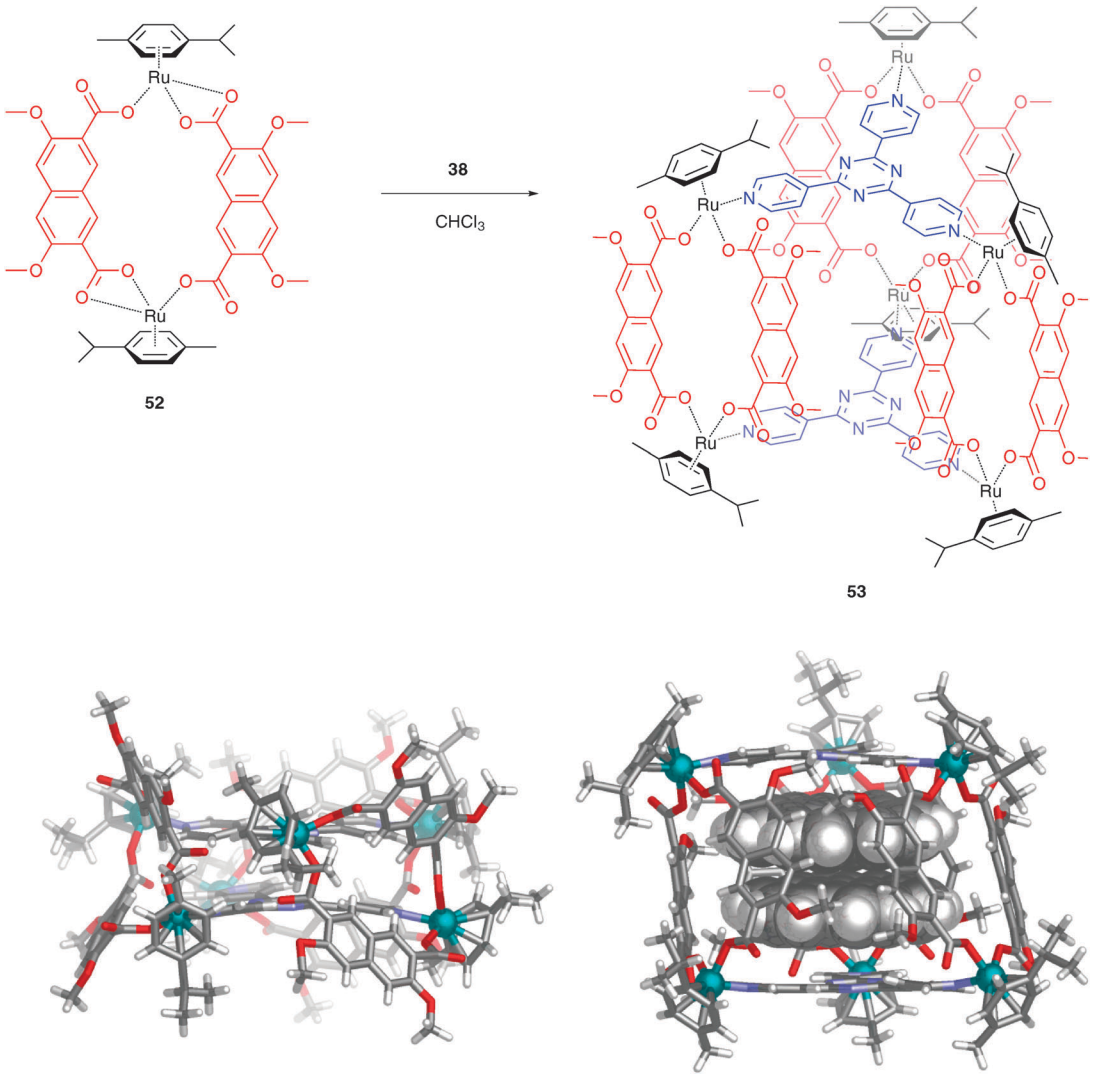

Fig. 14 Synthesis of heteroleptic cage **53** (top) and its crystal structure in the absence of coronene (bottom left) and presence of coronene (bottom right). Addition of coronene resulted in a dramatic change in the cage's geometry and concomitant increase in cavity volume.[56]

size of the host and the release of the guest was observed: as the size of the portal decreases, the release of guest was slowed down. This work illustrates how selective modification of particular ligands in a heteroleptic metal–organic cage allows fine-tuning of the cage's host–guest properties.

Severin *et al.* have also reported a heteroleptic, trigonal prismatic metal–organic cage based on Ru^{II} piano-stool corners.[56] The introduction of conformational freedom in the three ligands that define the pillars of the prismatic cage resulted in a cage with an adaptable cavity volume (Fig. 14).

Starting from dinuclear complex **52**, in which each of the metal centres is coordinated by both a monodentate carboxylate and a bidentate carboxylate, upon the addition of **38** (2 equivalents relative to 3 equivalents of **52**) in chloroform, cage **53** was prepared by the opening of the four-membered carboxylate-ruthenium chelate ring by one of the pyridyl moieties of **38**. Upon addition of coronene to cage **53**, it was observed that up to two equivalents of this guest were encapsulated in the cage's cavity. X-ray crystal structure determination of both the empty and the filled cage, revealed that encapsulation of two coronene molecules is accompanied by a dramatic change in geometry, which is facilitated by the conformational flexibility of the cage. Whereas for the empty cage, the distance between the top and bottom triazine ring is 3.4 Å, upon encapsulation of two coronene molecules this distance increases to 10.9 Å, corresponding to an increase of cavity volume from negligibly small to greater than 500 $Å^3$. Modulation of the cavity size was thus not a consequence of distortion of the ligand, but was the result of a more staggered conformation of the two triazine rings and concomitant increase in triazine–triazine distance.

Lee *et al.* have reported how three different (metallo)porphyrin building blocks can be assembled into a rigid, well-defined supramolecular box with catalytic properties (Fig. 15).[57] Previously, the authors showed that combining porphyrin building blocks **56** and **54** in a 2 : 4 ratio, resulted in the selective formation of supramolecular box **58**.[58] To prevent self-recognition (**56** with **56**, and **54** with **54**), orthogonal metalation of **56** with Sn^{IV} and **54** with Zn^{II} was employed. Moreover, torsional motion along the Zn–porphyrin–Zn axis was restricted by tethering each **56** subunit to a total of four zinc ions. The steric demand created

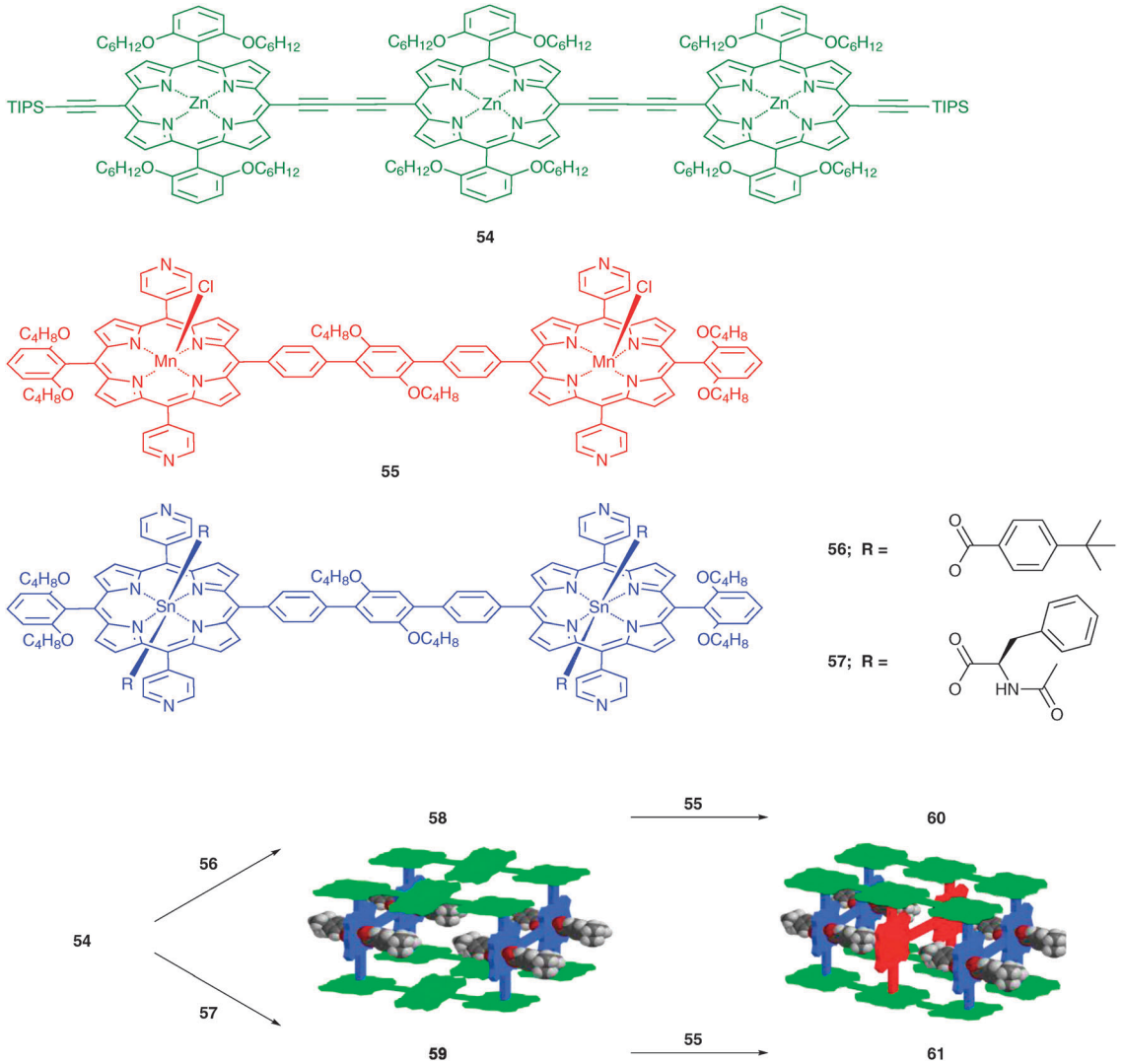

Fig. 15 Schematic representation of the self-assembly of the building blocks, **54**, **55** and **56** or **57**, into a catalytically active heteroleptic porphyrin box.[57]

by the axial ligands of the Sn^{IV} sites forced the **56** units to link selectively the first and third porphyrins of the **54** units, leaving the central Zn sites unoccupied, thereby defining a large cavity (22 × 14 × 10 Å).[58] The design of the two porphyrin building blocks was such that the smallest closed structure (fully zinc-ligated structure) that can be formed from **56** and **54** without strain is the orthogonally arranged assembly, **58**, in compliance with the principle of maximum site occupancy.[58]

In a subsequent contribution Lee *et al.* showed how a manganese porphyrin dimer **55** (with a sterically undemanding axial chloride ligand) could occupy the remaining sites in the **58** box, thus creating a three-component porphyrin box **60** with catalytic activity (Fig. 15).[57] Complex **60** could be prepared by addition of **55** to **58**, or in a one-pot synthesis from porphyrin building blocks **56**, **54** and **55**, illustrating the selectivity of this self-sorting process. Complex **60** was found to be a size-selective catalyst for the epoxidation of stilbenes: the epoxidation of *cis*-stilbene occurred 5.5 times faster than the sterically bulky *cis*-3,3′,5,5′-tetra(*tert*-butyl)stilbene. In addition, enantioselective catalysis could be achieved by formation of a chiral porphyrin box, **61**, which was achieved by replacing the achiral Sn^{IV} porphyrin dimer **56** for chiral analogue **57**. This chiral box was employed in the catalytic oxidation of methyl *p*-tolyl sulfide, resulting in methyl *p*-tolyl sulfoxide with 12% enantiomeric excess.

This work illustrates how control over three-dimensional organisation of three different porphyrin building blocks with appropriate functionalities can create tailored capsules with designed function.

Recently, both the groups of Stang[59] and Mukherjee[60] reported the selective preparation of heteroleptic three-component metal–organic assemblies, based on the principle of charge separation. Instead of relying solely on the coordination of a pyridinyl donor to an appropriate organoplatinum or an organo-palladium acceptor, they included a third component: a multitopic carboxylate. Stang and co-workers used a *cis*-protected platinum complex, in combination with both a pyridine-functionalised ligand and a carboxylate-functionalised ligand to prepare different three-component metallo-macrocycles as well as three-dimensional, trigonal or tetragonal prismatic, cages.[59]

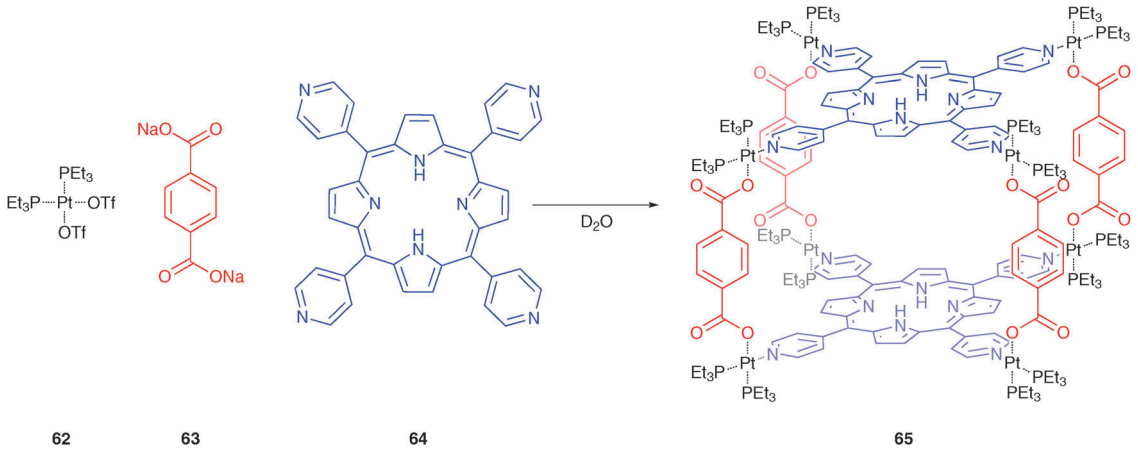

Fig. 16 Charge separation-driven self-assembly of dicarboxylate **63** and tetrapyridyl donor **64** in the presence of Pt^{II} salt **62** yielding heteroleptic cage **65**.[59]

For example, mixing Pt^{II} acceptor **62**, carboxylate ligand **63** and tetrapyridyl donor **64** in a 8 : 4 : 2 ratio, resulted in the formation of heteroleptic cage **65** as the major product (Fig. 16).

$^{31}P\{^{1}H\}$ NMR spectrometry on **65** revealed two coupled doublets, supporting the heteroleptic coordination environment. A computational study on a model Pt^{II} complex was performed in order to estimate the energy difference between homoleptic coordination and heteroleptic coordination (Fig. 17). Compared to the two homoleptic Pt^{II} complexes, the corresponding two heteroleptic species are favoured by 364.6 kJ mol^{-1}. The different electronic properties of carboxylate (negative) and pyridine (neutral) donors were cited as a driving force for heteroleptic coordination *via* charge separation. For the heteroleptic species only one, positively charged, pyridyl moiety is coordinated to each Pt^{II} centre; consequently, the charges can be separated and the electrostatic repulsion can be reduced.

Complex **65**, could also be prepared starting from the trigonal prism formed in the reaction between Pt^{II} acceptor **62** and tetrapyridyl donor **64** in a 6 : 3 ratio. To this homoleptic cage was added the (neutral) triangle Pt_3**63**$_3$ formed by **62** and carboxylate ligand **63**, which resulted in the breakdown of the two homoleptic species in favour of the heteroleptic cage **65**.

Bar *et al.* employed the concept of charge separation to prepare a trigonal prismatic Pd_6 complex.[60] The mixure of benzene-1,3,5-tricarboxylate (potassium salt) with a *cis*-protected Pd^{II} acceptor and 4,4′-bipyridine in a 2 : 6 : 3 ratio in water yielded the heteroleptic prismatic cage as the major product. When benzene-1,3,5-tricarboxylic acid was employed in the synthesis, the same Pd_6 cage was formed, but with two molecules of the triacid within the cavity.

Most reported self-assembled metal–organic complexes are the product of thermodynamically controlled assembly processes. Very recently, Barran, Lusby and co-workers reported a kinetically-controlled self-assembly strategy, in which the sequence of addition of the building blocks affected the stereochemistry of the final metallosupramolecular structure.[61] Relying on the *trans* effect, it was possible to create a single metal centre (Pt^{II}) possessing *cis*-exchangeable sites with different ligand exchange rates. This difference in kinetic behaviour opened up the route to two stereoisomeric trigonal prismatic cages, comprising two tris(4-pyridyl)triazine ligands (**38**), three 4,4′-bipyridine (**67**) ligands and six Pt^{II} centres, each with one phenyl and three pyridyl ligands (Fig. 18). In earlier work the authors had already shown that such a metallo-supramolecular trigonal prismatic cage could be prepared that

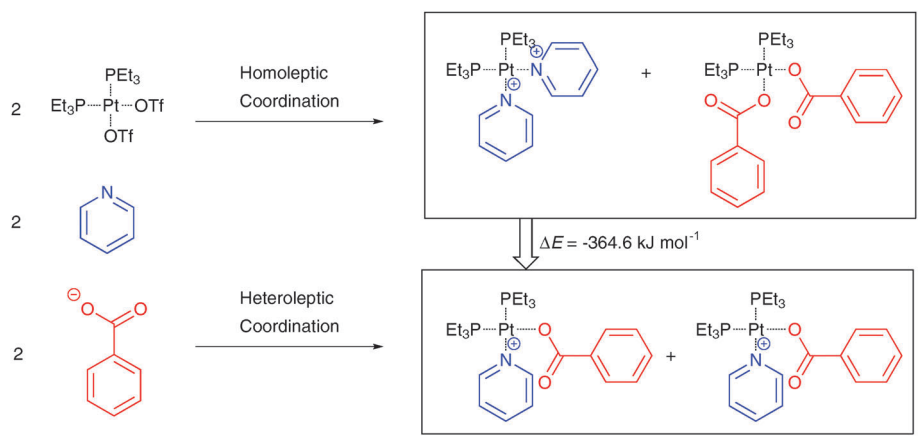

Fig. 17 Representation of selective self-assembly of *cis*-$Pt(PEt_3)_2(OTf)_2$ with carboxylate and pyridyl moieties due to the lower energy of the heteroleptic system.[59]

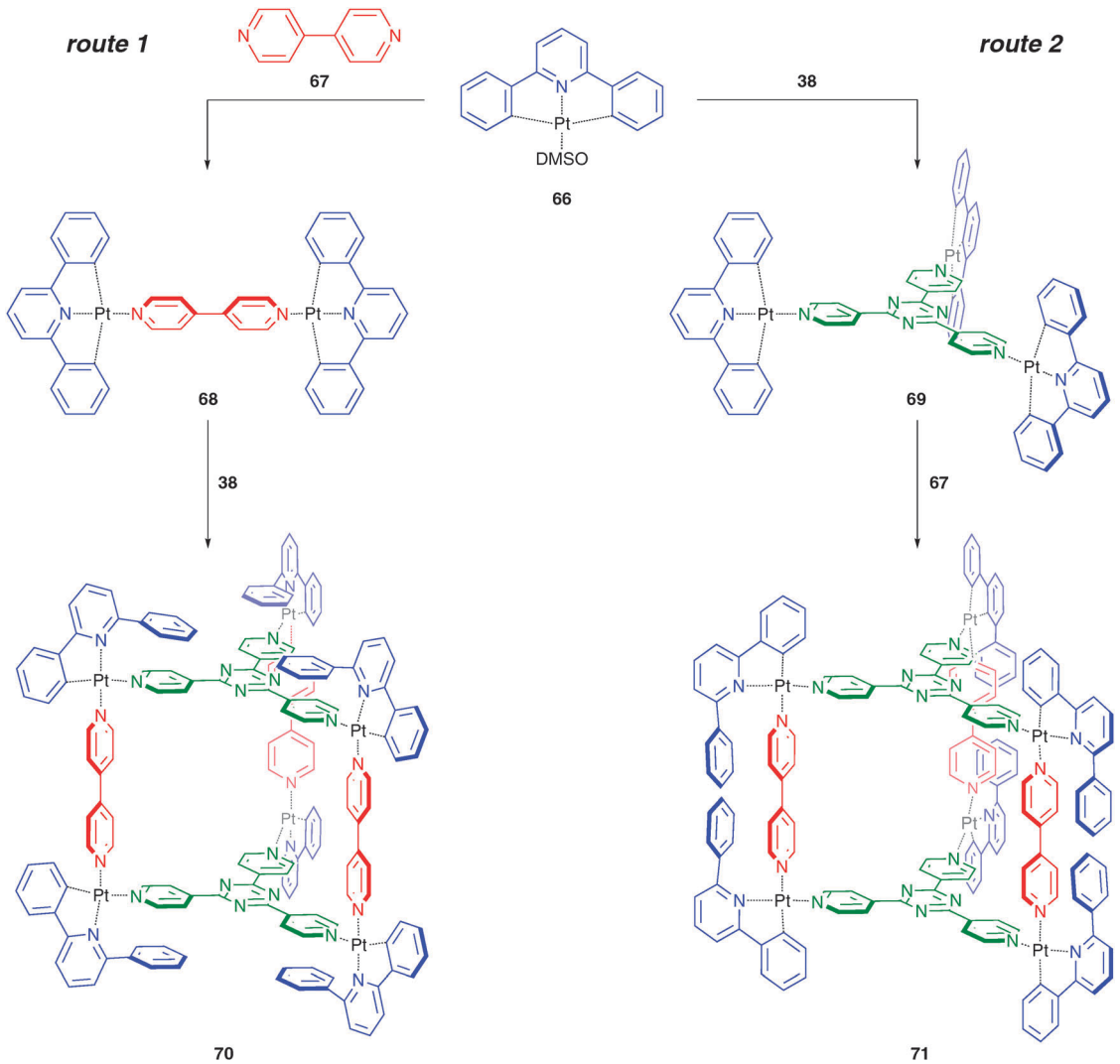

Fig. 18 Sequence-specific control of the formation of heteroleptic, diastereoisomeric cages **70** and **71**. Depending on the order of addition of **38** and **67**, the *cis* Pt_6 complex **70** (*via* route 1) or the *trans* Pt_6 complex **71** (*via* route 2) is formed.[61]

could be reversibly disassembled and reassembled by changing the pH.[62]

The order of addition of **38** and bipyridine ligand **67** to the Pt^{II} precursor, **66**, dictated whether the *cis* Pt_6 complex **70** (*i.e.* ligand **38** is coordinated *cis* to the nitrogen of the 2,6-diphenylpyridine ligand) or alternatively the *trans* Pt_6 complex **71** would be formed (Fig. 18).

^{1}H NMR revealed that for both routes 1 and 2 (Fig. 18) a single product was formed and that these two products were not identical. Although on the basis of the ^{1}H NMR spectra the stereochemistry of the product of each of the routes could be inferred, more direct evidence could be obtained from nanoelectrospray mass spectrometry (nESI). The collision-induced dissociation pathways differed significantly for the two products, enabling unequivocal assignment of the stereochemistry of each of the isomeric cages. Remarkably, the two stereoisomeric cages display such kinetic stability that even heating at 80 °C for 24 hours did not result in the conversion of the kinetic product into the thermodynamic one.

The work of Lusby and Barran underscores how the incorporation of coordination sites with different kinetic properties can be employed to create heteroleptic complexes with control over stereoisomerism. Moreover, their method does not rely on a template.

Schmittel *et al.* have developed a strategy based on both electronic and steric effects to control the coordination of two ligands with different coordination motifs around a single metal centre, such that only the preferred heteroleptic metal coordination is favoured.[63–65] Their methodology, referred to as the heteroleptic phenanthroline (HETPHEN) complexation concept, relies upon the combined coordination of a bulky 2,9-diarylphenanthroline and a sterically undemanding second ligand around a metal centre. As the homoleptic bisphenanthroline metal complex cannot be formed based on steric grounds, the heteroleptic metal complex is preferentially formed in order to achieve maximum site occupancy, despite its kinetic lability (Fig. 19A).

Previous work had already shown that this method could be employed to create trigonal prismatic cages, prepared from a C_3-symmetrical trifunctional terpyridine ligand and a bifunctional phenanthroline ligand in the presence of Zn^{II}, in a 2 : 3 : 6 ratio.[65] In more recent work, Schmittel and co-workers combined the

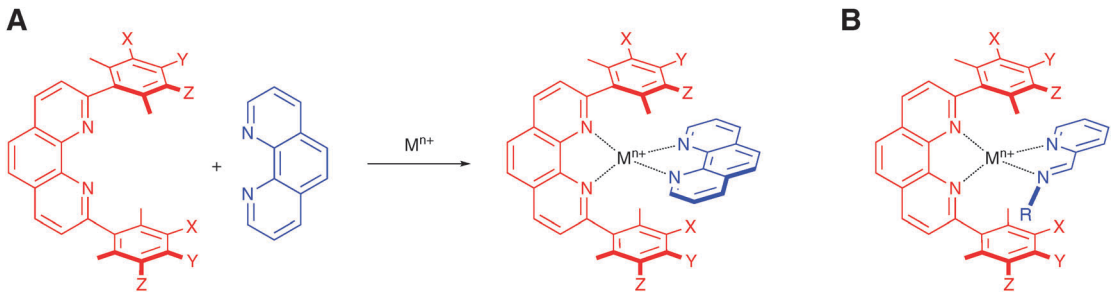

Fig. 19 Illustration of the HETPHEN concept and its extension to heteroleptic complexes involving pyridylimine.[64] Substituents X, Y and Z can be varied.

bulky phenanthroline ligand with a pyridylimine ligand, thus incorporating reversible imine bonds in the complex (Fig. 19B), which allowed them to synthesise a metal–organic capsule with three distinct compartments (Fig. 20).

Mixing ligands **72** and **73** in the presence of a Cu^{I} salt in a 2 : 3 : 6 ratio in CD_2Cl_2 yielded trigonal prismatic cage **74**. The six terminal aldehyde groups in **74** allowed post-self-assembly functionalisation by addition of six equivalents of toluidine (**75**), thus yielding cage **76**. Alternatively, instead of adding six equivalents of monofunctional amines, two equivalents of trifunctional amine **77**, resulted in the formation of cage **78**. Molecular modelling of **78** revealed the volume of the larger central cavity and the two outer cavities to be 4500 $Å^3$ and 940 $Å^3$, respectively.

4. Heterometallic structures

The use of more than one metal in the synthesis of three-dimensional complexes can be a successful strategy for the creation of complex and functional structures. Similarly to the way in which organic ligands can direct the formation of

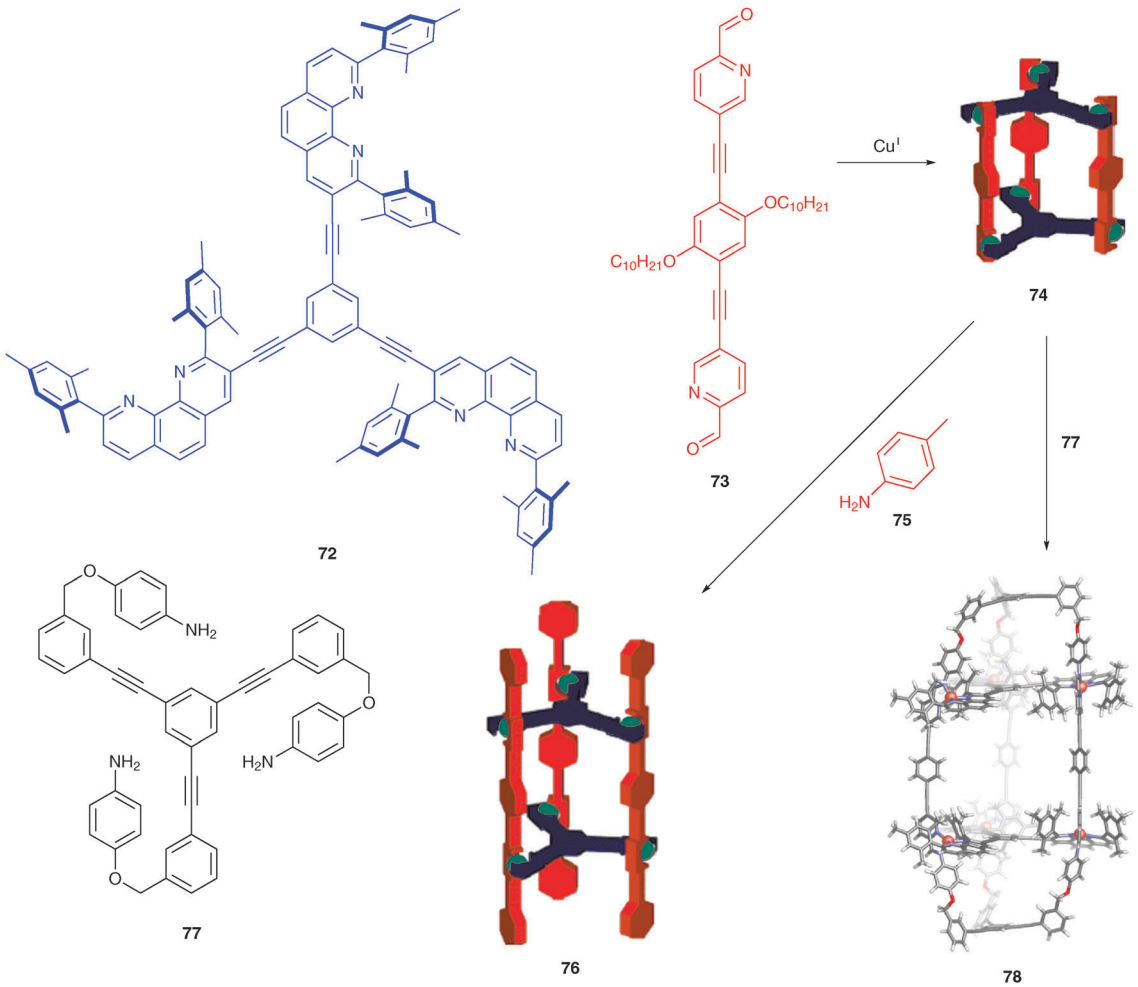

Fig. 20 Synthesis of heteroleptic cage **74**, which can be converted to cage **76** or three-compartment cage **78** by addition of **75** or **77**, respectively. Cage **78** is represented as its MM^{+} energy-minimised molecular model.[64]

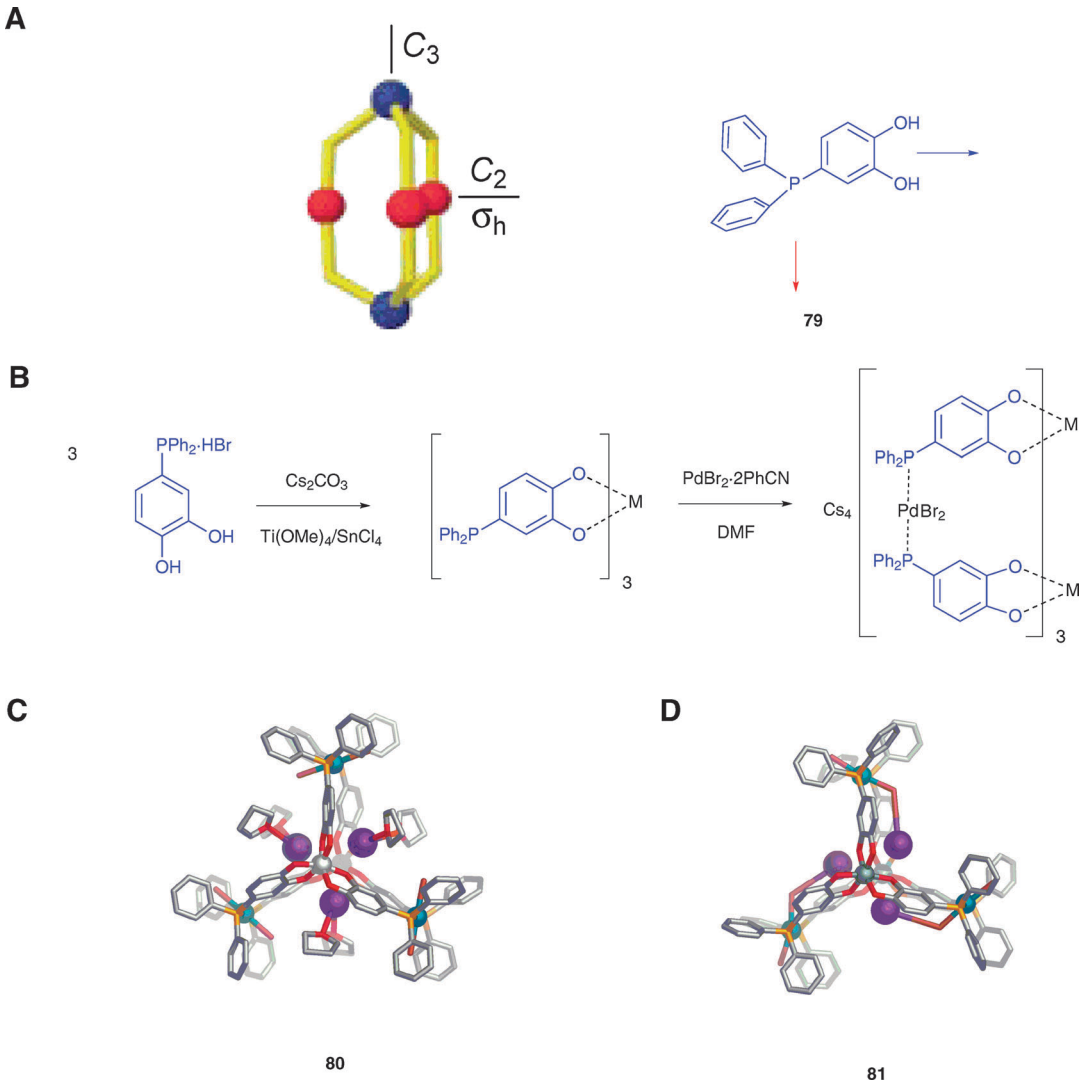

Fig. 21 (A) Depiction of the symmetry of subcomponents necessary for assembly of coordination-number incommensurate interactions and how **79** meets these requirements. (B) Multi-step synthesis of mesocate[71] structures: (C) crystal structures of **80** and (D) **81** showing encapsulated cesium ions. Cs atoms represented as purple spheres.

various discrete structures, through varying bond length, cation size, and coordination preference (as discussed above), the process of self-assembly can be controlled by the concerted use of two or more different metal ions having different coordination preferences.[66] The introduction of multiple metal sites also has the potential to introduce unique characteristics such as magnetic, photochemical or electrochemical properties and metal-centred chirality, whilst avoiding the potentially expensive, difficult and time-consuming multi-step synthesis that would be required to grant these properties through organic ligands. Such techniques have proven useful in the creation of two-dimensional assemblies in many cases,[67,68] but recently they have been extended to the investigation of three-dimensional structures.

As discussed above,[15] Raymond and co-workers have successfully developed a rational design for high-symmetry three-dimensional structures including helicates, mesocates and tetrahedra using "coordination number incommensurate interactions".[69,70] This involves the combination of an octahedral metal ion coordinated by three identical bidentate moieties to give a threefold symmetry axis with a symmetric multidentate ligand which contains the other symmetry element required to generate the structure (Fig. 21A). Wong, in collaboration with Raymond, has shown that with suitable ligands, mixed-metal systems can give the necessary symmetry elements for the formation of such structures (Fig. 21).[71] Ligand **79**, was designed which contained two metal binding sites, one soft and one hard, which can preferentially interact with one metal ion over another. The catechol functionality of **79** provides hard donor sites, forming tris-chelates with hard tri-valent metals, such as Ti^{IV} and Sn^{IV}. The reaction of three equivalents of **79** with a M^{IV} ion gives $[M(\mathbf{79})_3]^{2-}$. This species generates the C_3 axis needed for the formation of a structure through coordination number incommensurate interactions. To complete the formation of a discrete structure using this strategy a metal site which generates a C_2 axis or mirror plane is required. The phosphane moiety of **79** is a soft donor which gives the desired two-fold symmetry interaction site upon coordination to a square

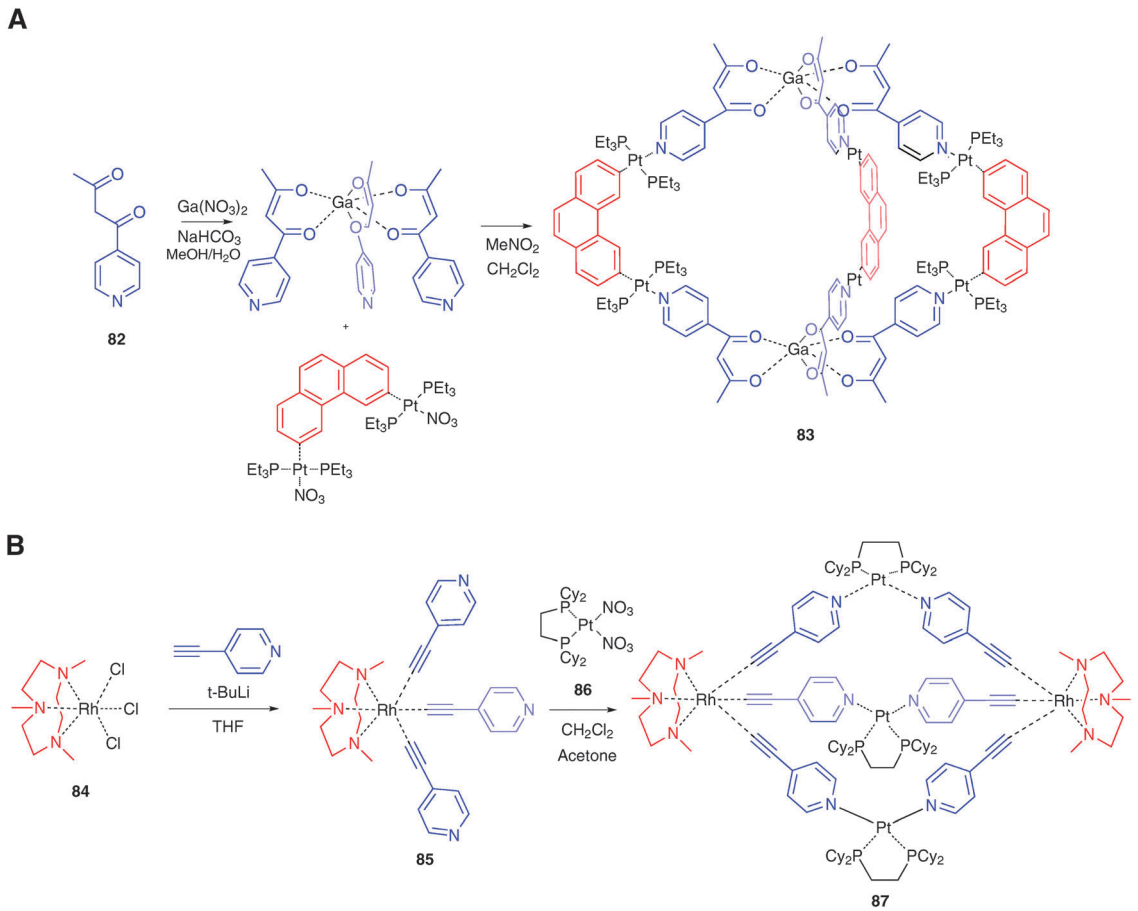

Fig. 22 (A) Heterotopic ligand **82**, and its reaction with a Ga^{II} to generate a metallo-ligand, which combined with a 60° Pt^{II} acceptor to form **83**.[73] (B) Formation of **87** *via* the formation first of **85**, and its subsequent reaction with a 90° Pt^{II} acceptor, **86**.[76]

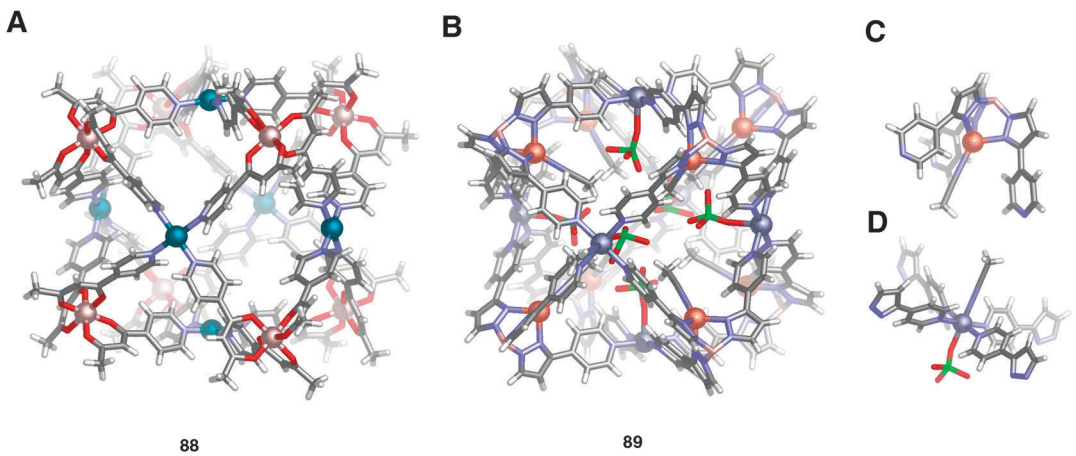

Fig. 23 (A) Crystal structure of **88**.[77] (B) Crystal structure of **89**, highlighting (C) the Cu^{I} coordination environments at each corner and (D) the coordination environment of the M^{II} ions on each face.[12]

planar metal ion (*e.g.* Pt^{II} or Pd^{II}) which has two of its coordination sites blocked, in this case by *trans* coordinating bromide anions. Generation of the $[M(\mathbf{79})_3]^{2-}$ metalloligand and its mixing with $Pd(PhCN)_2Br_2$ in DMF leads to the self-assembly of the $M_2M'_3L_6$ mesocate[72] structures **80** and **81**.

Different host guest-chemistry was observed depending on the mixture of metals used in combination with **79**. In the crystal structure of the titanium complex, **80**, a cesium counterion is buried within the complex, coordinated by four *endo*-catecholate oxygen atoms in a rectangular array and two molecules of THF. The tin complex, **81**, differs as a single bromine atom from each of the palladium centres replaces the THF molecules to complete the coordination of the cesium. This is possible in **81** as tin has a larger ionic radius that titanium, giving a longer metal–metal distance and a larger cavity.

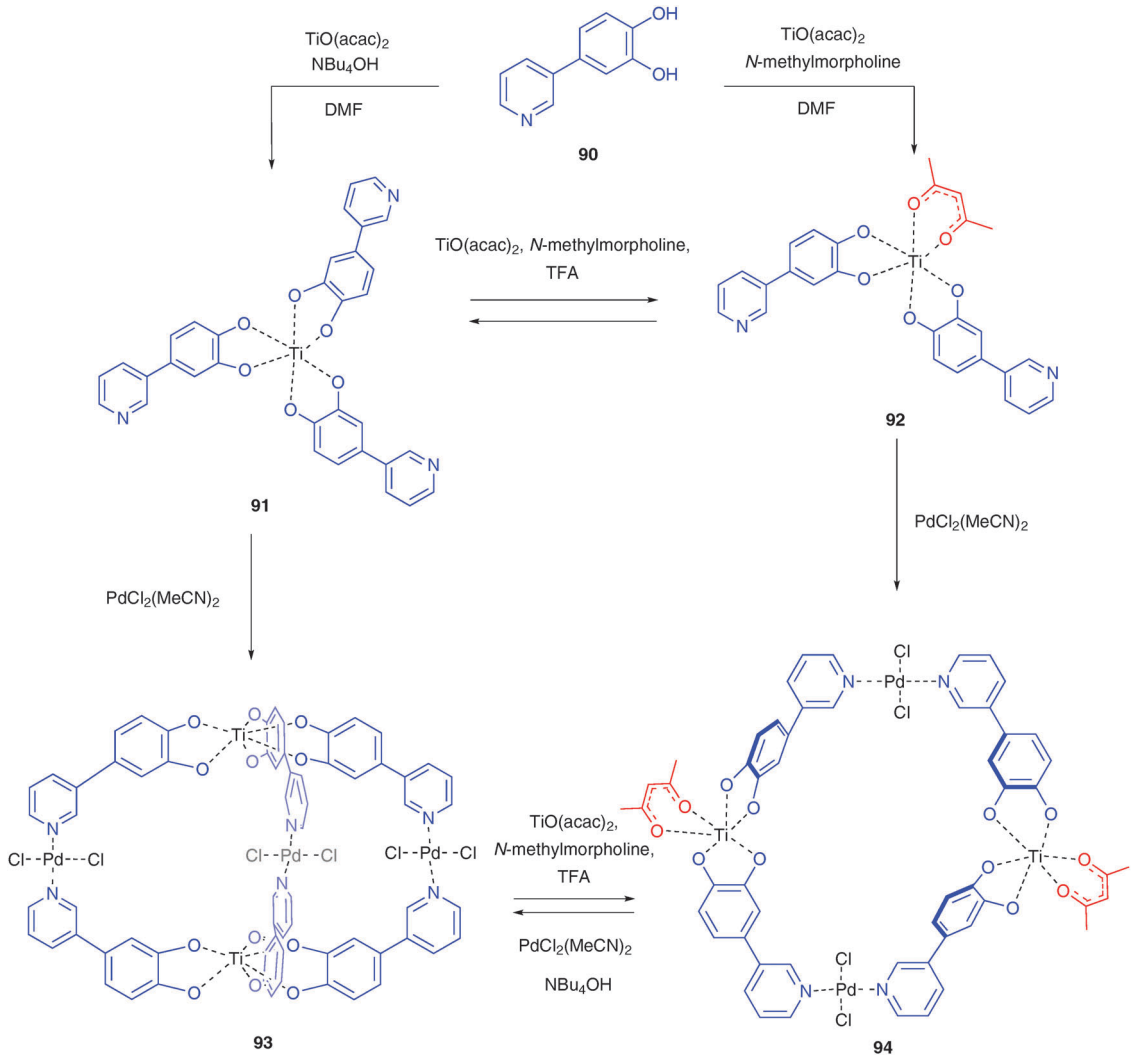

Fig. 24 pH-mediated switching between metalloligands **91** and **92** and between cage and macrocycle **93** and **94**.[79]

Stang and co-workers have designed a heterotopic ligand that shares key properties with **79**.[73] This ligand, **82**, incorporates a hard binding site, a β-diketone moiety able to coordinate to hard metal ions. The second binding site is a pyridine functional group, which has been used with success by Stang to create a wide variety of three-dimensional structures *via* coordination to square planar metal centres such as Pd^{II}.[74,75] Mixing 4-pyridylbutane-1,3-dione, **82**, with either Ga^{III} or Al^{III} leads to coordination of the metal cation by the β-diketone moiety, generating a tritopic metalloligand in which the three pyridyl motifs are arranged orthogonally to each other allowing for three-dimensional growth. By combining this with a ditopic platinum-containing subcomponent of either 90° or 60° geometry, three-dimensional structures were constructed (Fig. 22) as shown by ^{31}P and ^{1}H NMR spectroscopy and ESI-MS.

An alkyne-based heterotopic ligand has been used by Youngs and co-workers to create a trigonal bipyramidal cage.[76] By creating rhodium complex **84**, which is capped by an acetylide ligand in a *fac* conformation, and replacing the chloride ligands with acetylene ligands bearing suitably orientated pyridyl binding sites, tridentate metalloligand **85** is formed. The reaction of **85** with square planar $Pd(NO_3)_2$(1,2-bis(dicyclohexylphosphino)ethane), **86**, generated the cage structure **87**.

This two-step strategy has been shown to also work for the synthesis of larger polyhedra. Wu and co-workers combined **82** with Al^{III} to generate a similar metallo-ligand to the one shown in Fig. 22.[77] A trigonal bipyramidal structure similar to **83** was created by combination of this metalloligand with $ZnBr_2$. However, reaction of the complex with $Pd^{II}(NO_3)_2$ in the absence of any ancillary ligand led to the formation of a large cubic cage, **88**. In this structure the six Pd^{II} metal centres occupy the vertices of an octahedron with a metalloligand capping each face (Fig. 23A).

A similar cubic construct, **89**, (Fig. 23B) was synthesised by Batten and co-workers.[12] The threefold symmetry axes of this structure are in this case defined by the bifunctional ligand (tris[3-(4′-pyridyl)pyrazol-1-yl]hydroborate). Upon mixing this flexible ligand with Cu^{I}, a structurally rigid metalloligand is formed and the direction of the pyridyl binding sites is locked. Subsequent addition of divalent metal species ([MX_2] where M = Cu, Mn, Zn, Cd, Fe; X = ClO_4, NO_3, BF_4) leads to the formation of the 'nanoballs'. The three pyridine linkers

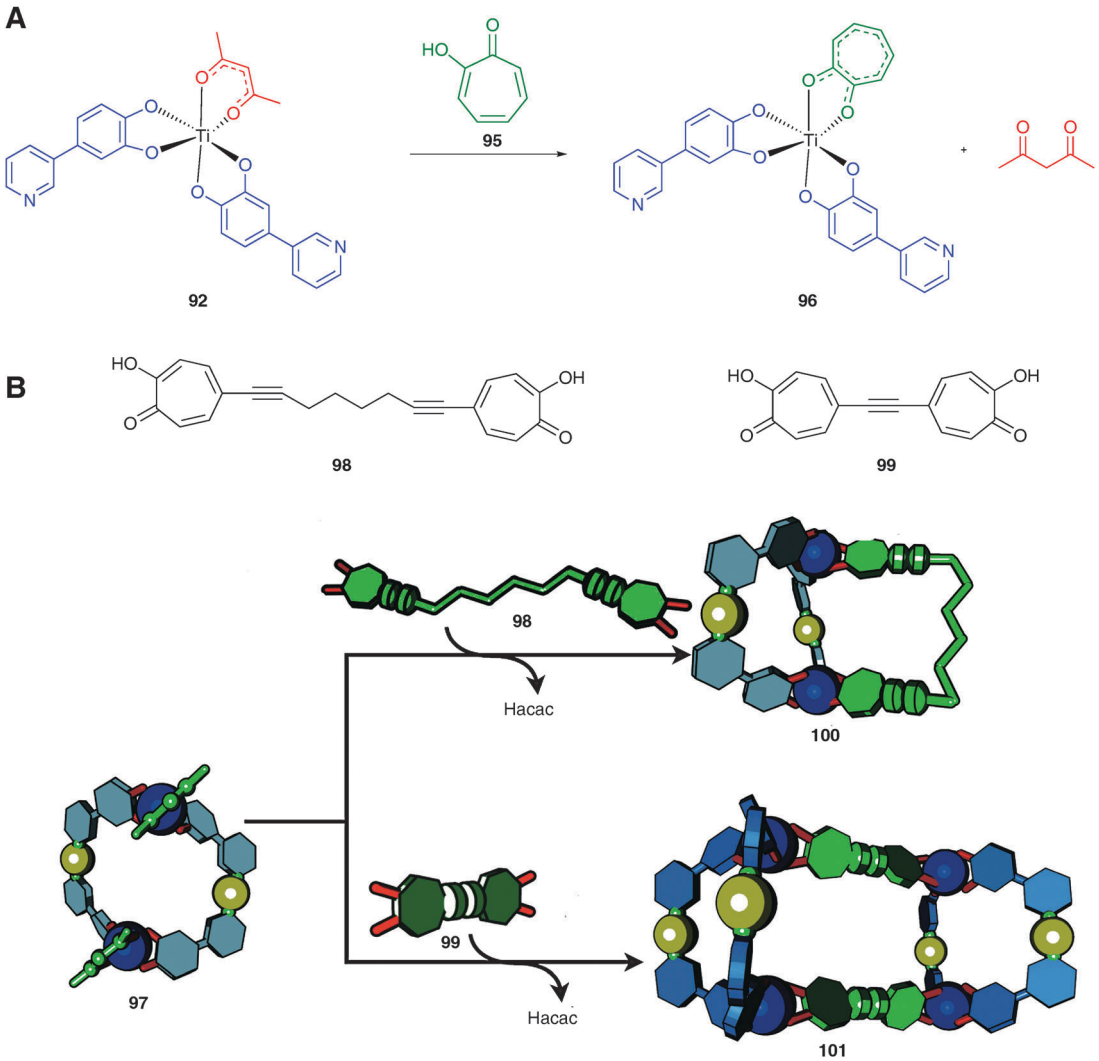

Fig. 25 (A) Displacement of acac by Htrop to generate new metalloligand **96**. (B) Formation of new three-dimensional structures by displacement of acac by bisbidentate ligands **98** and **99**.[78]

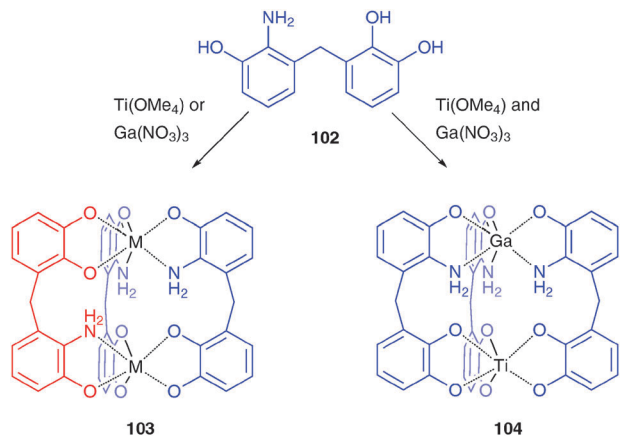

Fig. 26 Synthesis of monometallic helicate **103** and mixed-metal helicate **104**.[80]

on each ligand are connected to three additional ligands by an octahedral metal ion whose coordination environment is completed by anions or solvent molecules. The large pore sizes and internal volume of **89** provide space for gas and solvent encapsulation. The presence of labile metal ions on each face allows for increased access for gas molecules.

The mechanisms and programmability of the self-assembly of heterometallic systems have been investigated by Shionoya and co-workers.[78,79] A similar heterotopic ligand to those used above, **90**, bearing a hard catechol bidentate site and a relatively soft pyridine binding site, was employed to coordinate to Ti^{IV}. Upon mixing of **90** with $TiO(acac)_2$ and the strong base *n*-Bu_4NOH, ESI-MS showed the formation of both a tripodal metalloligand, **91**, composed of three ligands and one Ti^{IV} ion, as well as the presence of species **92**, in which Ti^{IV} is bound by one acac and two catecholato ligands. As the reaction proceeds, **92** is consumed, leaving **91** as the sole product. By performing this reaction in the presence of a weaker base, *N*-methylmorpholine, formation of **91** was almost completely suppressed. By changing the pH of the solution, it was possible to select either **91** or **92** as the product, allowing for the formation of cage **93** or ring **94** upon reaction with $PdCl_2(CH_3CN)_2$. Once formed, **93** and **94** could be interconverted in a similar manner to the metalloligands, with an alteration of pH leading to

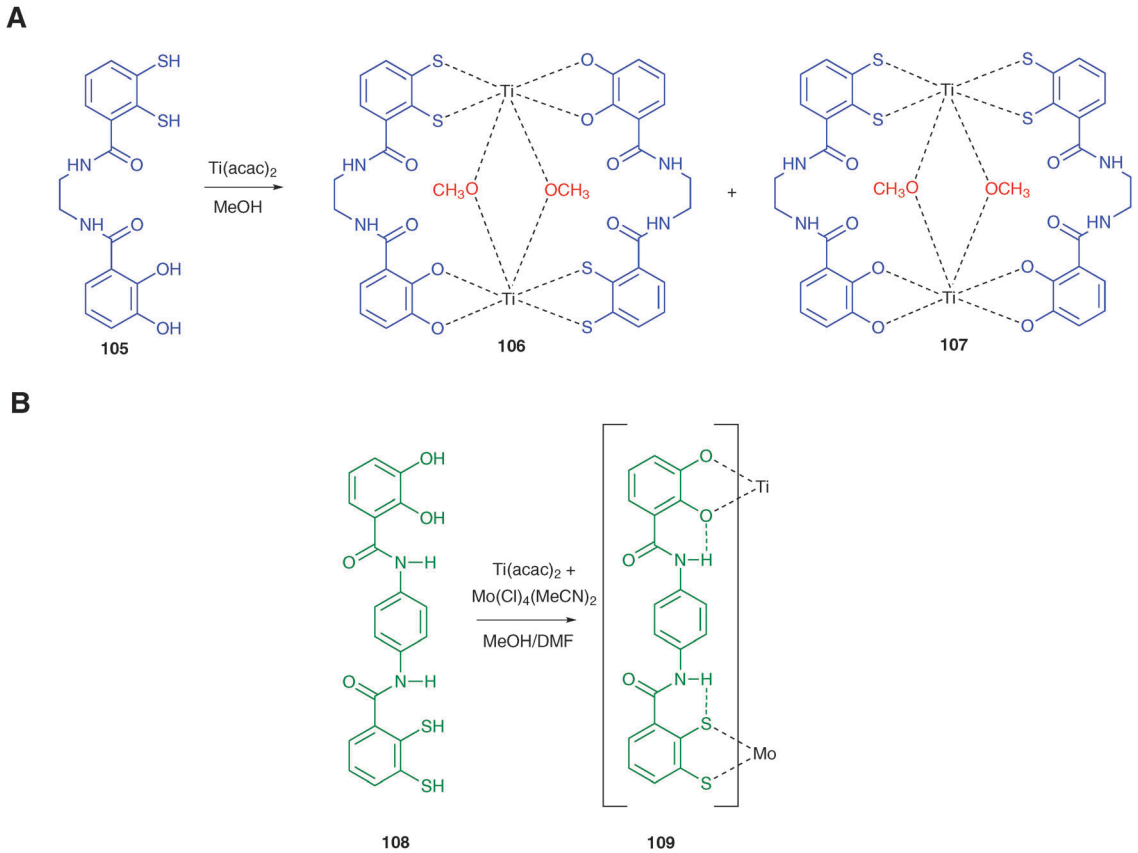

Fig. 27 (A) Mixture of ligand **105** with Ti^{IV} to give mixture of helicates, **106** and **107**. (B) Synthesis of mixed-metal helicate **109**.[81,82]

quantitative switching from one structure to the other (Fig. 24).

The Shionoya group has used ligand switching for the synthesis of increasingly complex three-dimensional structures. It was found that the acac ligand bound to the Ti^{IV} ion in **92** could be replaced by a similar hard bidentate ligand, tropolone (**95**), to form the more stable [Ti(**90**)$_2$(**95**)], **96**, in very high yields. These conversions also occurred with heterometallic Ti^{IV}/Pd^{II} assemblies (Fig. 25A). The displacement of acac, made possible by the lability of the titanium centre of the metalloligands, provides an excellent starting point for higher-order multi-component self-assembly. By pre-forming the heterometallic ring in which acac is bound to each titanium ion, bis-bidentate ligands containing trop-like moieties can be added to replace the acac ligand and lead to the formation of new discrete three-dimensional structures **100** and **101** (Fig. 25B).

The Pd^{II} metal centre within this ring does not interfere with the exchange processes occurring around the Ti^{IV} centre making it a suitable precursor from which such reactions can occur. The use of flexible linker **98** generates a tetranuclear structure, **100**, in which the ligand can bend around to form the smallest possible structure, as is favoured entropically. By using short and rigid ligand **99**, composed of two trop rings joined by an ethynyl linker, an elongated octanuclear complex, **101**, is formed.

In the heterometallic complexes mentioned previously in this section, a two-step process was used, whereby a metalloligand was first formed and then mixed with the second metal salt to generate the final structure. In the case of **100** and **101** the Shionoya group also sought to perform these syntheses in a one-pot reaction. Upon mixing all reagents in [D_7]DMF an insoluble precipitate was formed, as well as a low yield of the desired product. This precipitate was most likely an insoluble product deriving from Ti^{IV} and the trop ligands in an early stage of the reaction. Precipitation thus removed the subcomponents from solution, leaving them no longer available for the self-assembly process.

An example of a mixed-metal helicate comes from the group of Albrecht. A bis-bidentate ligand, **102**, was designed, having two electronically different binding sites. Mixing **102** with Ti^{IV} gives triple helicate **103**, wherein two of the ligands are orientated in one direction, with the third aligned in the opposite direction (Fig. 26). Upon mixing **102** with both Ga^{III} and Ti^{IV} in a 1 : 1 : 3 ratio all three ligands are arranged with the same directionality to give a C_3-symmetric complex, **104**, where one type of coordination site binds preferentially to the gallium, and the other to the titanium.[80] Here, the mixture of supramolecular precursors in different ratios provides access to two different structures.

In a similar example from Hahn *et al.*, mixed benzene-*o*-dithiol/catechol ligands were observed to react with Ti^{IV} to give dinuclear triple-stranded or dinuclear double-stranded helicates, depending on the backbone of the ligand used as well as the reaction conditions.[81–83] Mixing of ligand **105** with Ti^{IV} generates a helicate, but the directionality of these complexes resulted in mixtures of isomers in solution (Fig. 27A).

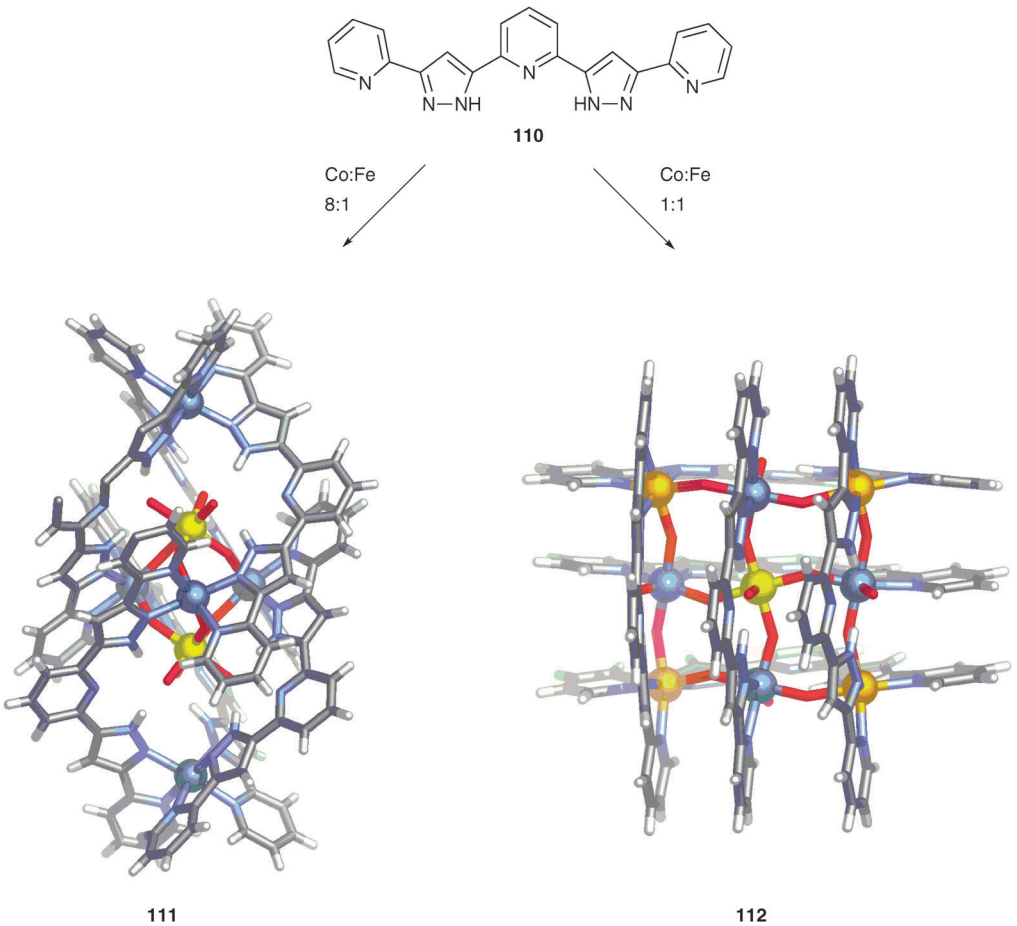

Fig. 28 Synthesis of **111** and **112** from the mixing of ligand **110** and differing ratios of Fe^{II} and Co^{II} salts.[84] Co^{II} blue, Fe^{II} orange and Fe^{III} yellow.

Mixture of the ligand, **108**, Ti^{IV} and Mo^{IV} in a 1 : 1 : 1 ratio leads to the formation of a mixed-metal triple-stranded helicate, **109**, in which the directionality of the ligands is all the same, and a racemic mixture of $\Delta\Delta/\Lambda\Lambda$ was observed in solution[82] (Fig. 27B). Coordination of the dithiol unit around the Mo^{IV} centre also allows for strong hydrogen bonding within the ligand due to a more planar arrangement of the ligands as compared to the $Ti(dithiol)_3$ unit, which is more severely twisted. Furthermore, the presence of the Mo^{IV} allows for potential electrochemical control over the final product formed as Mo^{VI} has a trigonal prismatic coordination geometry with dithiol coordination sites. This control is unique to heterometallic systems and emphasises their potential for the creation of systems with defined properties.

The groups of Oshio and Cronin have synthesised and characterised a polypyridine ligand (2,6-bis[5-(2-pyridinyl)-1*H*-pyrazole-3-yl]pyridine), **110**, which has one tridentate and two bidentate coordination sites.[84] This ligand has been shown to form a mixed Co^{II}/Co^{III} grid.[85] The group have developed structures incorporating both cobalt and iron. A heptanuclear helical complex, **111**, was formed by mixing $Fe(BF_4)_2$ and $Co(BF_4)_2$ in a 1 : 8 ratio with **110** and triethylamine in a mixture of acetonitrile and methanol. By changing the Fe : Co ratio to 1 : 1 a [3 × 3] grid, **112**, with six ligands coordinated to five iron and four cobalt ions is formed (Fig. 28).

Four Fe^{II} ions occupy the four corners of the grid, with a single Fe^{III} ion in the middle coordination site. The remaining four sites are occupied by Co^{II} ions. Each metal ion is linked to the adjacent metal by bridging μ_2-hydroxo ligands. The central, hard Fe^{III} ion is not a good match for the polypyridyl ligand and is in fact not bound by the tridentate binding site of the ligand, but coordinated to four bridging μ_2-hydroxo ligands and two terminal hydroxo ligands. These ligands hydrogen bond to the tridentate binding sites of the adjacent ligands.

A similar situation is seen in helical structure **111**. Here two Co^{II} ions are bound by three bidentate sites in an octahedral arrangement at each end of the helicate. There is a pentanuclear core within the helix, in which three Co^{II} ions are arranged in a planar arrangement, with μ_2-oxo bridges connecting two capping $[Fe^{III}O_3(OH_2)_3]^{3-}$ groups. Despite the rigid, planar nature of the ligand – properties that would ordinarily preclude the formation of a helicate – other factors predominate in the case of **111**. The Fe^{III} ions show a preference for an O_6 donor set and interact with **110** only through ligand hydrogen-bonding, whereas the Co^{II} ions favour the N_6 and N_4O_2 donor sets available to them through direct coordination to **110**. In **112** a similar situation is seen, but in this instance there are also Fe^{II} ions present that favour the N_4O_2 coordination environment available to them at the four corners of the grid.

Pyrogallol[4]arenes have been shown to form discrete hydrogen-bonded capsules in solution.[86] Atwood and co-workers have demonstrated that the addition of metal ions to solutions of suitable pyrogallol[4]arenes can lead to metal coordination replacing the

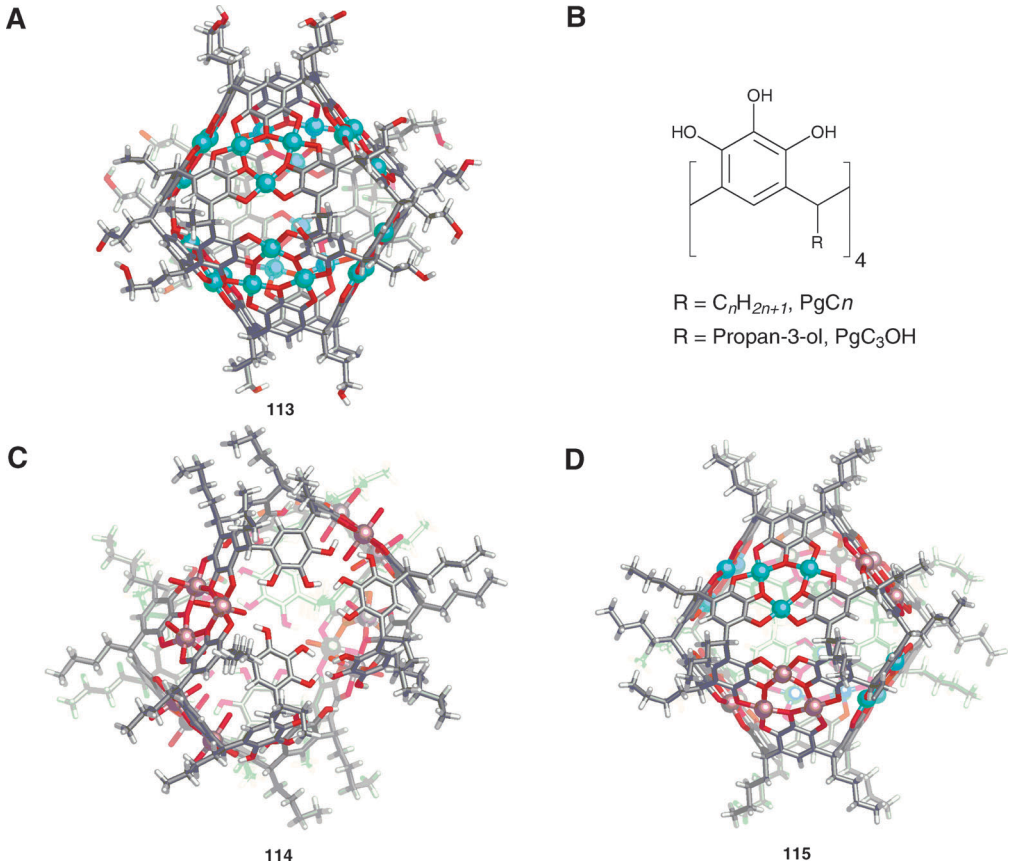

Fig. 29 (A) Structure, **113**, resulting from reaction of copper(II) nitrate with *C*-alkylpyrogallol[4]arenes.[88] (B) Examples of ligands used in these studies. (C) Distorted rugby-ball like structure **114**, formed upon mixing Ga^{III} with *C*-alkylpyrogallol[4]arenes.[90] (D) Mixed-metal structure **115** formed upon addition of Cu^{II} ions to **114**. Ga^{III} ions depicted as brown and Cu^{II} ions blue.

hydrogen bonds around the seams of the cages. These metallo-supramolecular complexes have different properties to the hydrogen-bond-directed analogues, including slower rates of guest uptake.[87] The reaction of an excess of a Cu^{II} salt with a solution of *C*-propan-3-olpyrogallol[4]arene gives a product, **113**, that is almost identical structurally to the hydrogen-bonded analogue (Fig. 29A).[88] In contrast, the addition of Ga^{III} cations to the same *C*-alkylpyrogallol[4]arenes gives complex **114**, which has a distorted rugby-ball shape (Fig. 29C).[89]

In the latter case only twelve metal ions are incorporated into the capsule, leaving uncoordinated hydrogen-bonding sites in the capsule framework. By replacing the protons forming these bonds with metal ions these capsules could be "stitched-up" and the structure altered. Addition of copper(II) nitrate to pre-formed crystals of **114** led to deprotonation of hydrogen-bond donors and their replacement by copper(II) ions, as well as displacement of some Ga^{III} centres, transforming the rugby-ball-shaped structure of the homometallic Ga^{III} capsule to give the more spherical heterometallic cage **115**, similar to the pure copper-linked and hydrogen-bonding analogues (Fig. 29D). Addition of a Zn^{II} salt to Ga^{III} capsules also leads to exchange of hydrogen bonds for coordination linkages, resulting in the incorporation of Zn^{II} into a hexameric capsule. This stucture cannot be synthesised using a mono-metallic approach,[90] as mixing of Zn^{II} with *C*-alkylpyrogallol[4]arenes in the absence of Ga^{III} leads to the formation of a dimeric monometallic species.[91]

The weak-link approach is a coordination-driven approach to the synthesis of supramolecular assemblies. It involves the use of bidentate binding motifs which contain one strong metal–phosphine bond and one weak bond, between a metal and an atom such as oxygen or sulfur. The weaker bonds can be broken by the addition of stronger coordinating ligands, allowing for transformation from one assembly into another. This approach has been used to create complex three-dimensional structures such as cylinders.[92] The addition of a bidentate ligand to a rhodium salt generated the macrocycle **116** which can be converted to expanded macrocycles **117** and **118** by the addition of CO and MeCN respectively. The carbon monoxide and acetonitrile ligands can be displaced by dinitrile and diisocyanide ligands, respectively, to give cylindrical structures **119** and **120** (Fig. 30).

A recent example from our group showing the power of self-assembly of complex structures using multiple metals, is the formation of **123** (Fig. 31).[93]

Coordination of a square planar Pt^{II} metal centre by 4-aminophenyl-pyridine creates a C_4-symmetric complex with an amino group at each corner. A tetra-bidentate ligand is

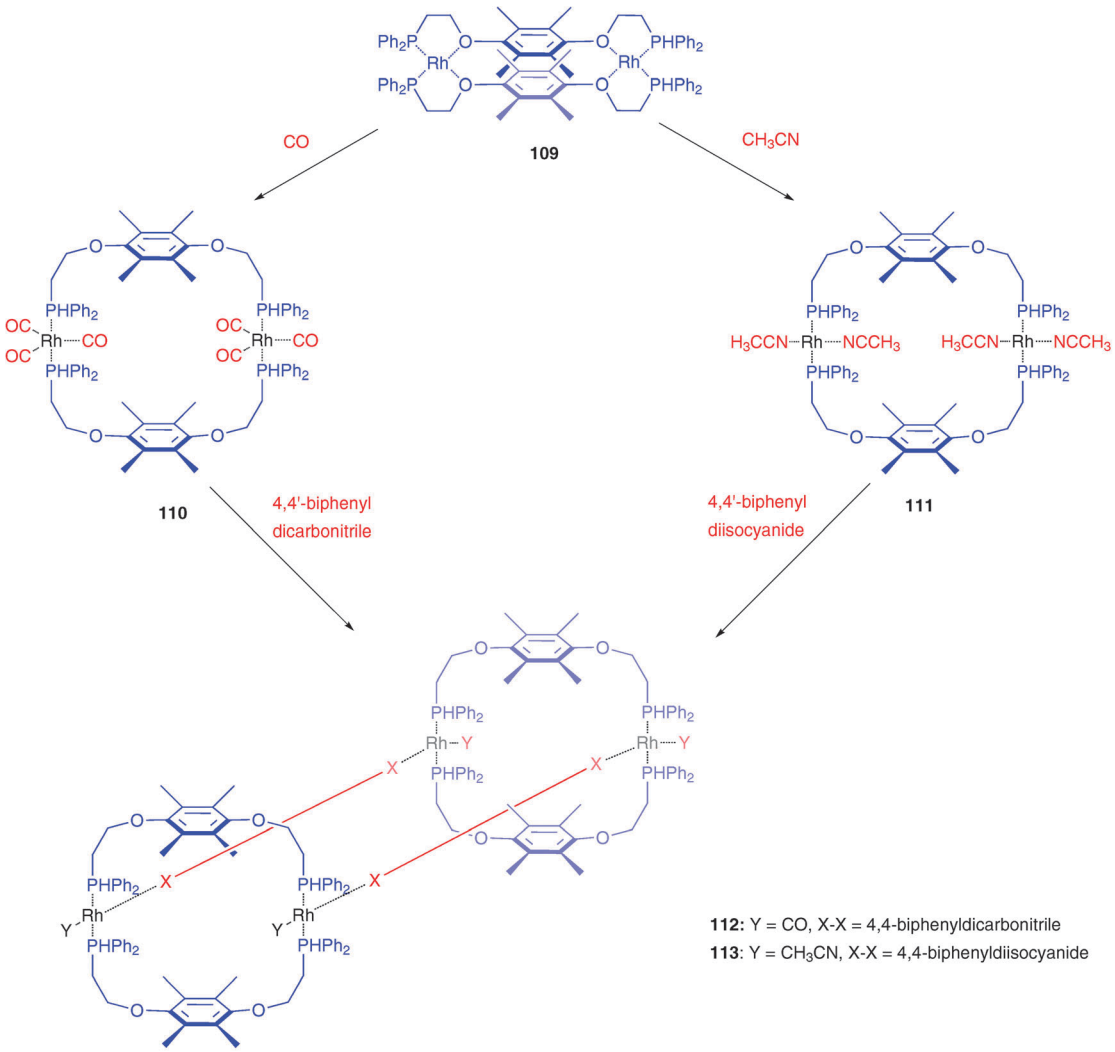

Fig. 30 Synthesis of cylindrical complexes **119** and **120** *via* the weak-link approach.[92]

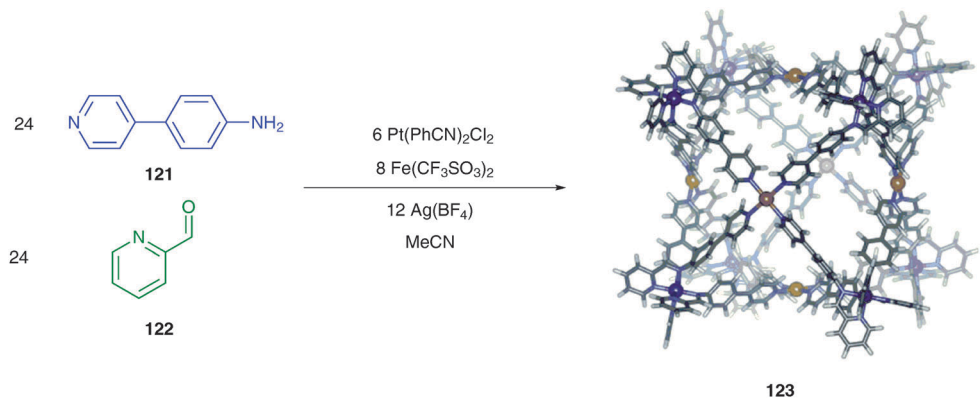

Fig. 31 Self-assembly of **123** from 62 subcomponents in an acetonitrile solution.[93]

formed by imine condensation upon the addition of 2-pyridinecarboxaldehyde and iron(II), generating a cube-like structure with octahedral Fe^{II} ions at each vertex and Pt^{II} ions capping each face.[93] However, **123** can also be synthesised in a one-pot reaction. The Pt^{II} ions coordinate preferentially to the pyridine functional groups, preventing their interaction with the Fe^{II} ions, and the dynamic nature of the imine and coordination bonds allows for error checking, leading to the isolation of **123** as the final thermodynamic product from the initial mixture of 62 subcomponents, with 96 new bonds being formed.

5. Conclusion and outlook

As outlined above, the design and synthesis of three-dimensional metal–organic supramolecular architectures is a field in which there has been much recent innovation. The reversible interactions that govern the formation of self-assembled complexes have allowed for the development of synthetic methods for increasingly complicated structures. By building upon work which has come before in the design of Archimedean and Platonic solids, a diverse set of rules has been deciphered, utilising strategies such as templates and asymmetric ligands, as well as combining multiple ligands and metals to create single product structures.

The new functions and applications of these structures fuel interest in them, together with the intellectual challenge of understanding, exploiting and directing the selectivity of multiple different bond-forming reactions in parallel. The preparation of these structures thus remains a fertile ground for opportunity and creativity.

Acknowledgements

We thank Dr T. K. Ronson, Dr A. Sallas and Dr A. Stefankiewicz for critical reading of the manuscript. The Engineering and Physical Sciences Research Council (I.A.R. & J.R.N.), the Netherlands Organisation for Scientific Research (M.M.J.S.) and the DYNAMOL initial training network of the 7th EU Framework Program (C.B.) are acknowledged for financial support.

References

1 R. Chakrabarty, P. S. Mukherjee and P. J. Stang, *Chem. Rev.*, 2011, **111**, 6810–6918.
2 S. Leininger, B. Olenyuk and P. J. Stang, *Chem. Rev.*, 2000, **100**, 853–908.
3 S. J. Dalgarno, N. P. Power and J. L. Atwood, *Coord. Chem. Rev.*, 2008, **252**, 825–841.
4 T. D. Hamilton, G. S. Papaefstathiou and L. R. MacGillivray, *J. Solid State Chem.*, 2005, **178**, 2409–2413.
5 S. R. Seidel and P. J. Stang, *Acc. Chem. Res.*, 2002, **35**, 972–983.
6 M. Yoshizawa, J. K. Klosterman and M. Fujita, *Angew. Chem., Int. Ed.*, 2009, **48**, 3418–3438.
7 P. Mal, B. Breiner, K. Rissanen and J. R. Nitschke, *Science*, 2009, **324**, 1697–1699.
8 M. M. J. Smulders and J. R. Nitschke, *Chem. Sci.*, 2012, **3**, 785–788.
9 C. J. Hastings, M. D. Pluth, R. G. Bergman and K. N. Raymond, *J. Am. Chem. Soc.*, 2010, **132**, 6938–6940.
10 T. Murase, S. Horiuchi and M. Fujita, *J. Am. Chem. Soc.*, 2010, **132**, 2866–2867.
11 I. A. Riddell, M. M. J. Smulders, J. K. Clegg and J. R. Nitschke, *Chem. Commun.*, 2011, **47**, 457–459.
12 M. B. Duriska, S. M. Neville, J. Lu, S. S. Iremonger, J. F. Boas, C. J. Kepert and S. R. Batten, *Angew. Chem., Int. Ed.*, 2009, **48**, 8919–8922.
13 Y. R. Hristova, M. M. J. Smulders, J. K. Clegg, B. Breiner and J. R. Nitschke, *Chem. Sci.*, 2011, **2**, 638–641.
14 S. Turega, M. Whitehead, B. R. Hall, M. F. Haddow, C. A. Hunter and M. D. Ward, *Chem. Commun.*, 2012, **48**, 2752–2754.
15 D. L. Caulder and K. N. Raymond, *Acc. Chem. Res.*, 1999, **32**, 975–982.
16 P. J. Stang and B. Olenyuk, *Acc. Chem. Res.*, 1997, **30**, 502–518.
17 D. Tranchemontagne, Z. Ni, M. O'Keeffe and O. Yaghi, *Angew. Chem., Int. Ed.*, 2008, **47**, 5136–5147.
18 X. Feng, X. Ding and D. Jiang, *Chem. Soc. Rev.*, 2012, **41**, 6010–6022.
19 A. Rit, T. Pape, A. Hepp and F. E. Hahn, *Organometallics*, 2011, **30**, 334–347.
20 M. Schmidtendorf, T. Pape and F. E. Hahn, *Angew. Chem., Int. Ed.*, 2012, **51**, 2195–2198.
21 Q.-F. Sun, J. Iwasa, D. Ogawa, Y. Ishido, S. Sato, T. Ozeki, Y. Sei, K. Yamaguchi and M. Fujita, *Science*, 2010, **328**, 1144–1147.
22 M. Tominaga, K. Suzuki, M. Kawano, T. Kusukawa, T. Ozeki, S. Sakamoto, K. Yamaguchi and M. Fujita, *Angew. Chem., Int. Ed.*, 2004, **43**, 5621–5625.
23 J. Bunzen, J. Iwasa, P. Bonakdarzadeh, E. Numata, K. Rissanen, S. Sato and M. Fujita, *Angew. Chem., Int. Ed.*, 2012, **51**, 3161–3163.
24 D. Fujita, A. Takahashi, S. Sato and M. Fujita, *J. Am. Chem. Soc.*, 2011, **133**, 13317–13319.
25 D. Moon, S. Kang, J. Park, K. Lee, R. P. John, H. Won, G. H. Seong, Y. S. Kim, G. H. Kim, H. Rhee and M. S. Lah, *J. Am. Chem. Soc.*, 2006, **128**, 3530–3531.
26 M. D. Ward, *Chem. Commun.*, 2009, 4487–4499.
27 I. S. Tidmarsh, T. B. Faust, H. Adams, L. P. Harding, L. Russo, W. Clegg and M. D. Ward, *J. Am. Chem. Soc.*, 2008, **130**, 15167–15175.
28 A. Stephenson and M. D. Ward, *Dalton Trans.*, 2011, **40**, 7824–7826.
29 I. A. Riddell, M. M. J. Smulders, J. K. Clegg, Y. R. Hristova, B. Breiner, J. D. Thoburn and J. R. Nitschke, *Nat. Chem.*, 2012, **4**, 751–756.
30 W. Xuan, M. Zhang, Y. Liu, Z. Chen and Y. Cui, *J. Am. Chem. Soc.*, 2012, **134**, 6904–6907.
31 M. Fukuda, R. Sekiya and R. Kuroda, *Angew. Chem., Int. Ed.*, 2008, **47**, 706–710.
32 S. Freye, J. Hey, A. Torras-Galán, D. Stalke, R. Herbst-Irmer, M. John and G. H. Clever, *Angew. Chem., Int. Ed.*, 2012, **51**, 2191–2194.
33 T. K. Ronson, J. Fisher, L. P. Harding, P. J. Rizkallah, J. E. Warren and M. J. Hardie, *Nat. Chem.*, 2009, **1**, 212–216.
34 S. Cardona-Serra, E. Coronado, P. Gavina, J. Ponce and S. Tatay, *Chem. Commun.*, 2011, **47**, 8235–8237.
35 J. Klingele, J. F. Boas, J. R. Pilbrow, B. Moubaraki, K. S. Murray, K. J. Berry, K. A. Hunter, G. B. Jameson, P. D. W. Boyd and S. Brooker, *Dalton Trans.*, 2007, 633–645.
36 C. Piguet, G. Bernardinelli and G. Hopfgartner, *Chem. Rev.*, 1997, **97**, 2005–2062.
37 M. C. O'Sullivan, J. K. Sprafke, D. V. Kondratuk, C. Rinfray, T. D. W. Claridge, A. Saywell, M. O. Blunt, J. N. O'Shea, P. H. Beton, M. Malfois and H. L. Anderson, *Nature*, 2011, **469**, 72–75.
38 T. Ross Kelly, R. L. Xie, C. Kraebel Weinreb and T. Bregant, *Tetrahedron Lett.*, 1998, **39**, 3675–3678.
39 D. V. Kondratuk, L. M. A. Perdigao, M. C. O'Sullivan, S. Svatek, G. Smith, J. N. O'Shea, P. H. Beton and H. L. Anderson, *Angew. Chem., Int. Ed.*, 2012, **51**, 6696–6699.
40 S. De, K. Mahata and M. Schmittel, *Chem. Soc. Rev.*, 2010, **39**, 1555–1575.
41 P. Baxter, J.-M. Lehn, A. Decian and J. Fischer, *Angew. Chem., Int. Ed. Engl.*, 1993, **32**, 69–72.
42 P. N. W. Baxter, J.-M. Lehn, B. O. Kneisel, G. Baum and D. Fenske, *Chem.–Eur. J.*, 1999, **5**, 113–120.
43 R. Kramer, J.-M. Lehn and A. Marquis-Rigault, *Proc. Natl. Acad. Sci. U. S. A.*, 1993, **90**, 5394–5398.
44 S. Hiraoka, Y. Kubota and M. Fujita, *Chem. Commun.*, 2000, 1509–1510.
45 K. Kumazawa, K. Biradha, T. Kusukawa, T. Okano and M. Fujita, *Angew. Chem., Int. Ed.*, 2003, **42**, 3909–3913.
46 M. Fujita, D. Oguro, M. Miyazawa, H. Oka, K. Yamaguchi and K. Ogura, *Nature*, 1995, **378**, 469–471.
47 Y. Yamauchi, M. Yoshizawa, M. Akita and M. Fujita, *J. Am. Chem. Soc.*, 2009, **132**, 960–966.
48 K. Ono, M. Yoshizawa, M. Akita, T. Kato, Y. Tsunobuchi, S.-i. Ohkoshi and M. Fujita, *J. Am. Chem. Soc.*, 2009, **131**, 2782–2783.
49 T. Osuga, T. Murase, K. Ono, Y. Yamauchi and M. Fujita, *J. Am. Chem. Soc.*, 2010, **132**, 15553–15555.
50 M. Kiguchi, T. Takahashi, Y. Takahashi, Y. Yamauchi, T. Murase, M. Fujita, T. Tada and S. Watanabe, *Angew. Chem., Int. Ed.*, 2011, **50**, 5708–5711.

51 Y. Yamauchi, M. Yoshizawa, M. Akita and M. Fujita, *Proc. Natl. Acad. Sci. U. S. A.*, 2009, **106**, 10435–10437.
52 N. P. E. Barry, O. Zava, P. J. Dyson and B. Therrien, *Chem.–Eur. J.*, 2011, **17**, 9669–9677.
53 B. Therrien, *Eur. J. Inorg. Chem.*, 2009, **2009**, 2445–2453.
54 J. Mattsson, P. Govindaswamy, J. Furrer, Y. Sei, K. Yamaguchi, G. Süss-Fink and B. Therrien, *Organometallics*, 2008, **27**, 4346–4356.
55 B. Therrien, G. Süss-Fink, P. Govindaswamy, A. K. Renfrew and P. J. Dyson, *Angew. Chem., Int. Ed.*, 2008, **47**, 3773–3776.
56 S. Mirtschin, A. Slabon-Turski, R. Scopelliti, A. H. Velders and K. Severin, *J. Am. Chem. Soc.*, 2010, **132**, 14004–14005.
57 S. J. Lee, S.-H. Cho, K. L. Mulfort, D. M. Tiede, J. T. Hupp and S. T. Nguyen, *J. Am. Chem. Soc.*, 2008, **130**, 16828–16829.
58 S. J. Lee, K. L. Mulfort, X. Zuo, A. J. Goshe, P. J. Wesson, S. T. Nguyen, J. T. Hupp and D. M. Tiede, *J. Am. Chem. Soc.*, 2007, **130**, 836–838.
59 Y.-R. Zheng, Z. Zhao, M. Wang, K. Ghosh, J. B. Pollock, T. R. Cook and P. J. Stang, *J. Am. Chem. Soc.*, 2010, **132**, 16873–16882.
60 A. K. Bar, G. Mostafa and P. S. Mukherjee, *Inorg. Chem.*, 2010, **49**, 7647–7649.
61 O. Chepelin, J. Ujma, P. E. Barran and P. J. Lusby, *Angew. Chem., Int. Ed.*, 2012, **51**, 4194–4197.
62 P. J. Lusby, P. Müller, S. J. Pike and A. M. Z. Slawin, *J. Am. Chem. Soc.*, 2009, **131**, 16398–16400.
63 J. Fan, M. Lal Saha, B. Song, H. Schönherr and M. Schmittel, *J. Am. Chem. Soc.*, 2012, **134**, 150–153.
64 M. Schmittel, M. L. Saha and J. Fan, *Org. Lett.*, 2011, **13**, 3916–3919.
65 M. Schmittel and B. He, *Chem. Commun.*, 2008, 4723–4725.
66 V. D. Vreshch, A. B. Lysenko, A. N. Chernega, J. A. K. Howard, H. Krautscheid, J. Sieler and K. V. Domasevitch, *Dalton Trans.*, 2004, 2899–2903.
67 K. Mahata and M. Schmittel, *J. Am. Chem. Soc.*, 2009, **131**, 16544–16554.
68 A. Petitjean, N. Kyritsakas and J.-M. Lehn, *Chem. Commun.*, 2004, 1168–1169.
69 D. L. Caulder, R. E. Powers, T. N. Parac and K. N. Raymond, *Angew. Chem., Int. Ed.*, 1998, **37**, 1840–1843.
70 C. Brückner, R. E. Powers and K. N. Raymond, *Angew. Chem., Int. Ed.*, 1998, **37**, 1837–1839.
71 X. Sun, D. W. Johnson, D. L. Caulder, R. E. Powers, K. N. Raymond and E. H. Wong, *Angew. Chem., Int. Ed.*, 1999, **38**, 1303–1307.
72 D. L. Caulder and K. N. Raymond, *J. Chem. Soc., Dalton Trans.*, 1999, 1185–1200.
73 M. Wang, V. Vajpayee, S. Shanmugaraju, Y.-R. Zheng, Z. Zhao, H. Kim, P. S. Mukherjee, K.-W. Chi and P. J. Stang, *Inorg. Chem.*, 2011, **50**, 1506–1512.
74 B. Olenyuk, J. A. Whiteford, A. Fechtenkötter and P. J. Stang, *Nature*, 1999, **398**, 796–799.
75 Y.-R. Zheng, Z. Zhao, H. Kim, M. Wang, K. Ghosh, J. B. Pollock, K.-W. Chi and P. J. Stang, *Inorg. Chem.*, 2010, **49**, 10238–10240.
76 J. C. Garrison, M. J. Panzner, P. D. Custer, D. V. Reddy, P. L. Rinaldi, C. A. Tessier and W. J. Youngs, *Chem. Commun.*, 2006, 4644–4646.
77 H.-B. Wu and Q.-M. Wang, *Angew. Chem., Int. Ed.*, 2009, **48**, 7343–7345.
78 Y. Sakata, S. Hiraoka and M. Shionoya, *Chem.–Eur. J.*, 2010, **16**, 3318–3325.
79 S. Hiraoka, Y. Sakata and M. Shionoya, *J. Am. Chem. Soc.*, 2008, **130**, 10058–10059.
80 M. Albrecht and R. Fröhlich, *J. Am. Chem. Soc.*, 1997, **119**, 1656–1661.
81 C. Schulze Isfort, T. Kreickmann, T. Pape, R. Fröhlich and F. E. Hahn, *Chem.–Eur. J.*, 2007, **13**, 2344–2357.
82 F. E. Hahn, M. Offermann, C. Schulze Isfort, T. Pape and R. Fröhlich, *Angew. Chem., Int. Ed.*, 2008, **47**, 6794–6797.
83 T. Kreickmann and F. E. Hahn, *Chem. Commun.*, 2007, 1111–1120.
84 G. N. Newton, T. Onuki, T. Shiga, M. Noguchi, T. Matsumoto, J. S. Mathieson, M. Nihei, M. Nakano, L. Cronin and H. Oshio, *Angew. Chem., Int. Ed.*, 2011, **50**, 4844–4848.
85 T. Shiga, T. Matsumoto, M. Noguchi, T. Onuki, N. Hoshino, G. N. Newton, M. Nakano and H. Oshio, *Chem.–Asian J.*, 2009, **4**, 1660–1663.
86 J. L. Atwood, L. J. Barbour and A. Jerga, *Chem. Commun.*, 2001, 2376–2377.
87 P. Jin, S. J. Dalgarno, C. Barnes, S. J. Teat and J. L. Atwood, *J. Am. Chem. Soc.*, 2008, **130**, 17262–17263.
88 S. J. Dalgarno, N. P. Power, J. E. Warren and J. L. Atwood, *Chem. Commun.*, 2008, 1539–1541.
89 R. M. McKinlay, P. K. Thallapally, G. W. V. Cave and J. L. Atwood, *Angew. Chem., Int. Ed.*, 2005, **44**, 5733–5736.
90 P. Jin, S. J. Dalgarno, J. E. Warren, S. J. Teat and J. L. Atwood, *Chem. Commun.*, 2009, 3348–3350.
91 N. P. Power, S. J. Dalgarno and J. L. Atwood, *New J. Chem.*, 2007, **31**, 17–20.
92 J. R. Farrell, C. A. Mirkin, L. M. Liable-Sands and A. L. Rheingold, *J. Am. Chem. Soc.*, 1998, **120**, 11834–11835.
93 M. M. J. Smulders, A. Jiménez and J. R. Nitschke, *Angew. Chem., Int. Ed.*, 2012, **51**, 6681–6685.

